www.sciencemag.org/cgi/content/full/science.1235822/DC1

Supplementary Materials for

Activation of the Yeast Hippo Pathway by Phosphorylation-Dependent Assembly of Signaling Complexes

Jeremy M. Rock, Daniel Lim, Lasse Stach, Roksana W. Ogrodowicz, Jamie M. Keck, Michele H. Jones, Catherine C. L. Wong, John R. Yates III, Mark Winey, Stephen J. Smerdon, Michael B. Yaffe, Angelika Amon*

*Corresponding author. E-mail: angelika@mit.edu

Published 11 April 2013 on *Science* Express
DOI: 10.1126/science.1235822

This PDF file includes:

Supplemental Online Materials

Materials and Methods

Media

YEP (yeast extract peptone) was supplemented with either 2% glucose (D), raffinose (R), or raffinose and galactose (RG). SC (synthetic medium) lacking appropriate amino acids for selection was used where indicated. CSM (complete synthetic medium) lacking or containing appropriate amino acids for selection or induction/repression of the *MET3* promoter was used where indicated.

Growth conditions

Fig. 1A-B and 4F: cells were arrested in G1 with α-factor pheromone (5 µg/ml) in YEPD medium at room temperature. 30 minutes prior to release the cells were shifted to 37°C. When the arrest was complete (after 3 hours), cells were released into pheromone free YEPD medium at 37°C. After 65 minutes, α-factor pheromone (10 µg/ml) was re-added to prevent entry into the subsequent cell cycle. The percentage of cells with metaphase spindles, anaphase spindles, 3HA-Cdc14 released from the nucleolus, the amount of Dbf2-associated kinase activity and immunoprecipitated 3MYC-Dbf2 was determined at the indicated times.

Fig. 1C: cells were grown to log phase in SC-Leu medium. Mob1 localization was analyzed in anaphase cells after a brief paraformaldehyde fixation ($n \geq 100$ cells).

Fig. 1D: cells were grown to log phase in YEPD medium and Mob1 localization was analyzed as in Fig. 1C.

Fig. 1E and 4E: cells were grown overnight in YEPR and spotted on YEPD or YEPRG plates and incubated at room temperature (YEPRG) or 37°C (YEPD). Approximately 3 X 10^4 cells were deposited in the first spot and each subsequent spot is a 10-fold serial dilution.

Fig. 2A: cells were arrested in anaphase by incubating them at 37°C for 2 hours and Nud1-3V5 was immunoprecipitated.

Fig. 2B: cells were grown to log phase in YEPD supplemented with 8 mM methioinine. Cells were then shifted to CSM-methionine medium for 60 minutes to induce expression of the *CDC15-SPB* fusion. Cdc15 and Mob1 localization was analyzed in G1/S, metaphase and anaphase cells after a brief paraformaldehyde fixation (n ≥ 100 cells).

Fig. 2C: cells were arrested in G1 with α-factor pheromone (5 µg/ml) in YEPD medium at room temperature. When the arrest was complete (after 2.5 hours), cells were released into pheromone free YEPD medium at room temperature to determine phosphorylation of Nud1 T78 (α-pT78), S63 (α-pS63), S53 (α-pS53) and total Nud1 levels as well as the percentage of cells in metaphase and anaphase. After 65 minutes, α-factor pheromone (10 µg/ml) was readded to prevent entry into the subsequent cell cycle.

Fig. 2D: cells were arrested in anaphase in YEPD medium at 37°C for 2 hours to determine phosphorylation of Nud1 T78 (α-pT78), S63 (α-pS63), S53 (α-pS53) and total Nud1 levels.

Fig. 2E: cells were arrested in S phase with hydroxyurea (200 mM) in YEPD supplemented with 8 mM methionine. When the arrest was complete (after 2 hours), cells were transferred into CSM-methionine medium containing glucose and hydroxyurea to induce Cdc15-SPB expression and phosphorylation of Nud1 T78 (α-pT78), S63 (α-pS63), S53 (α-pS53) and total Nud1 levels were determined.

Fig. 3A and 4D: cells were grown to log phase in YEPD and Mob1 localization was analyzed as in Fig. 1C.

Fig. 3B: cells were grown in YEPD medium for 2 hours at room temperature followed by incubation at 37°C for 2 hours. Note: the *mob1-77* allele is not very temperature sensitive in the W303 strain background. Thus, it was necessary to place the *mob1-77* allele under the control of *GAL1-10* promoter and simultaneously inhibit expression and incubate cells at the restrictive temperature of 37°C to achieve *mob1* loss-of-function.

Fig. 4H: cells were spotted on YEPD + 8 mM methioinine, CSM - methionine + glucose, or CSM - methionine + raffinose and galactose and incubated at 30°C. Approximately 3

X 10^4 cells were deposited in the first spot and each subsequent spot is a 10-fold serial dilution.

Fig. 4I: cells were arrested in G1 with α-factor (5 µg/ml) in YEPRaff medium + 8 mM methionine. One hour prior to release, cells were shifted to CSM medium - methionine + raffinose + α-factor to induce expression of the Mob1-Nud1 fusion. Cells were then released into CSM medium - methionine + raffinose. After 70 minutes, α-factor pheromone (10 µg/ml) was re-added to prevent entry into the subsequent cell cycle. After 145 minutes, galactose was added (arrow) to induce expression of *GAL-TEV1*. The percentage of cells with anaphase spindles was determined at the indicated times.

Yeast strains and plasmids

All strains are derivatives of W303 (A2587) and are listed in Table S2. All plasmids used in this study are listed in Table S3.

Plasmids:

NUD1-3V5, *GAL-NUD1*, *GAL-nud1*, *DBF2-eGFP*, and *DBF2-mTomato* fusions were constructed using standard PCR-based methods (*1, 2*). The *SPC72-CNM67* allele was a gift from Elmar Schiebel (*3*).

pA1921: *NUD1-3V5* was amplified with primers (5'-aataCTGCAGCGACATTGCTAAAAACATTC-3') and (5'-aataGAGCTCGATCTAATGCAGCTTTATTATCAAG-3') from strain A24513 genomic DNA. The resulting PCR product was cloned into the PstI and SacI sites of YIplac204. This cloning generated a *NUD1-3V5* allele driven from the *NUD1* promoter.

pA1931: a *nud1* gene fragment (from the AflII to ClaI sites of the endogenous gene) containing the indicated phosphorylation site mutations (Table S1) was synthesized by Mr. Gene. This gene fragment was then subcloned into the AflII-ClaI sites of plasmid pA1921. This cloning generated a *nud1-27A-3V5* phospho-mutant allele driven from the *NUD1* promoter.

pA1998: a *nud1* gene fragment (from the AflII to ClaI sites of the endogenous gene) containing the indicated phosphorylation site mutations (Table S1) was synthesized by

Mr. Gene. This gene fragment was then subcloned into the AflII-ClaI sites of plasmid pA1921. This cloning generated a *nud1-38A-3V5* phospho-mutant allele driven from the *NUD1* promoter. The additional four phosphorylation site mutations were generated by site-directed mutagenesis to generate the *nud1-42A-3V5* phospho-mutant allele.

pA2192: *MOB1-eGFP-NUD1* was cloned under the control of the *MET3* promoter using the following strategy. The *MET3* promoter was amplified with primers (5'-TTACGCCAAGCTTGCATGCCTGCAGGTCGACTCTAGAGGATGAAACTGAGTAAGATGCTCAGAATAC-3') and (5'-AAAAGAAAATAGCAACATACAAATTTTGTAGAAAAGACATCCTAGGGTTAATTATACTTTATTCTTG-3') using a *MET3* promoter containing plasmid as template; *MOB1-eGFP* was amplified with primers (5'-ATGTCTTTTCTACAAAATTTGTATG-3') and (5'-GCCACCACCAGAGCCACCTCCACCAGAACCTCCACCACCTAGTTTGTACAATTCATCAATACCATG-3') with A24631 genomic DNA as template; the *NUD1* N-terminus was amplified with primers (5'-CTAGGTGGTGGAGGTTCTGGTGGAGGTGGCTCTGGTGGTGGCATGGATATGGATACGCAGGAG-3') and (5'-TGTCACTAAGGTTTAGCACTAATAC-3') with plasmid 1921 as template; and the *NUD1* C-terminus was amplified with primers (5'-AAATCCTGAAAGTTGACCTATC -3') and (5'-TAAAACGACGGCCAGTGAATTCGAGCTCGGTACCCGGGGAGATCTAATGCAGCTTTATTATCAAG -3') with plasmid 1921 as template. Plasmid YCplac22 was digested with BamHI (*4*). Approximately equimolar amounts of BamHI-digested plasmid YCplac22 and each of the four PCR products above were cotransformed into yeast strain A2587. Homologous recombination between YCplac22 and the four PCR fragments generated the *pMET3-MOB1-eGFP-NUD1* allele. Plasmids were recovered from the resulting Trp+ colonies and by sequencing confirmed to contain mutation-free *pMET3-MOB1-eGFP-NUD1. pMET3-MOB1-eGFP-NUD1* was then subcloned into the HindIII and EcoRI sites of YIplac211 (*4*).

All other *nud1* and *mob1* mutant alleles were generated by site-directed mutagenesis.

NUD1 phospho-mutant allele analysis

Construction of strains to examine the effects of nud1-42A on exit from mitosis

Despite wild-type expression levels and localization patterns, the *nud1-42A* allele was not able to complement the temperature sensitive lethality of cells harboring the conditional *nud1-44* allele and in fact was synthetic lethal with this allele at the permissive temperature. Thus, to examine the effects of the *nud1-42A* allele on MEN activity we placed the temperature sensitive *nud1-44* allele under the control of the galactose-inducible/glucose-repressible *GAL1-10* promoter to generate a *GAL-nud1-44 nud1-42A* strain. *GAL-nud1-44 nud1-42A* cells, like MEN loss-of-function mutants, arrested in late anaphase when grown in glucose-containing medium at 37°C, the restrictive condition for the *GAL-nud1-44* allele (Fig. S1E and F).

Construction of strains to examine the effects of nud1-42A on MEN component localization

To perform MEN component localization studies in *nud1-42A* cells, we needed to generate a strain in which *nud1-42A* was the sole source of *NUD1* in the cell. The reason such a strain was desired was that we had previously observed intragenic complementation between the *nud1-42A* and *cdc18-1* alleles (data not shown; *cdc18-1* is a temperature sensitive allele of *NUD1*, (*5*)). A strain in which *nud1-42A* was the sole source of *NUD1* in the cell would obviate concerns that any observed MEN component localization to SPBs was the result of intragenic complementation, be it partial or complete. We succeeded in constructing a strain with *nud1-42A* as the sole source of *NUD1* by simultaneously introducing a constitutively active Dbf2 allele (*DBF2-HyA*) to activate the MEN and by restoring astral microtubule anchorage by expressing an *SPC72-CNM67* fusion into cells (*3, 6*). It should be noted that the suppression of the lethality of a *nud1-42A* allele by the combination of a constitutively active *DBF2* allele and a *SPC72-CNM67* allele indicates that the two major defects associated with the *nud1-42A* allele are MEN activation and astral microtubule organization. The coexpression of *DBF2-HyA* and *SPC72-CNM67* in otherwise wild-type cells did not perturb MEN component localization.

Generation of the nud1 phosphorylation site mutants described in Figure S3

GAL-nud1(42A) and *GAL-NUD1* alleles were constructed using standard PCR-based methods (*2*). Genomic DNA of yeast strains containing the *GAL-nud1(42A)* or *GAL-NUD1* alleles was isolated. PCR primers were designed such that the upstream primer was anchored at the selectable maker linked to the *GAL1-10* promoter and the

downstream primers were tiled across the *NUD1* or *nud1(42A)* alleles. The *GAL-nud1(42A)*-derived PCR products were then transformed into a wild-type strain diploid for *NUD1*, thus generating a pool of strains which contain a single wild-type *NUD1* allele and a tiled variant containing a variable number of phosphorylation site mutations derived from the *nud1(42A)* allele. The *GAL-NUD1*-derived PCR products were then transformed into a strain containing both a wild-type allele of *NUD1* and the *nud1(42A)* allele, thus generating a pool of strains which contain a single wild-type *NUD1* allele and a tiled variant containing a variable number of restored phosphorylation sites derived from the wild type *NUD1* allele.

To define the phosphorylation sites required for Dbf2-Mob1 SPB recruitment, we took advantage of the fact that overexpression of the *nud1-42A* allele causes lethality (Fig. S3A and C). *GAL-nud1-42A* cells arrested in anaphase with Cdc14 sequestered in the nucleolus indicating that the overexpressed nud1-42A protein interferes with MEN function. We created *NUD1* alleles harboring a subset of phosphorylation site mutants and identified critical residues by virtue of whether or not they caused lethality when overexpressed (Fig. S3).

Generation of NUD1 phosphomimetic mutants

We attempted to generate *NUD1* alleles where S53, S63 and/or T78 were replaced with the Asp or Glu to mimic the phosphorylated state of the three residues. As observed with many other proteins, these mutations did not effectively mimic phosphorylation and led to loss of *NUD1* function with respect to Mob1 localization to SPBs. Thus, rather than creating hyperactive alleles of *NUD1* these changes disrupted protein function in a manner that led to *NUD1* loss of function.

Fluorescence microscopy

Indirect *in situ* immunofluorescence methods to detect Tub1 were performed as previously described (*7*). V5 tagged proteins were detected with an anti-V5 antibody (Invitrogen) at a 1:1000 dilution. HA tagged proteins were detected with an anti-HA antibody (Covance) at a 1:150 dilution. Imaging of Bfa1-GFP, Tem1-GFP, Cdc15-eGFP, Cdc15-eGFP-Cnm67, Dbf2-eGFP, Dbf2-tdTomato, Mob1-eGFP, Mob1-mCherry, Mob1-eGFP-Cnm67, GFP-Tub1, mCherry-Tub1, Spc42-mCherry, and Spc72-eGFP cells were

performed as described previously (*8*). In all localization experiments, ≥ 100 cells were counted.

Live cell imaging

Cells were grown overnight in complete synthetic medium and transferred to a microfluidic chamber (CellASIC Corp. Hayward, CA). Cells were imaged using a Zeiss Axio Observer-Z1 with a 100X objective (NA=1.45), equipped with a Hamamatsu ORCA-ER digital camera. 11 Z-stacks (1 micron apart) were acquired and maximally projected. Metamorph software was used for image acquisition and processing.

Co-immunoprecipitation assays

For Dbf2-Mob1 co-immunoprecipitation, approximately 12 OD_{600} units of cells were collected, washed once with 50 mM Tris-Cl (pH 7.5), and then lysed with glass beads in a bead mill with lysis buffer (50 mM Tris-Cl at pH 7.5, 150 mM NaCl, 1% NP-40, 60 mM β-glycerolphosphate, 0.1 mM sodium orthovanadate, 15 mM para-nitrophenlylphosphate, 1 mM DTT, complete protease inhibitor cocktail [Roche]). 20 µl of anti-HA affinity matrix (Roche) was added to 1 mg of total protein and incubated for 2 hours. Beads were then washed six times with wash buffer (50 mM Tris-Cl at pH 7.5, 150 mM NaCl, 1% NP-40). Nud1 - Mob1 co-immunoprecipitation assays were performed as in (*3*).

Cdc15 kinase assays

cdc14-3 GAL-CDC15-3HA (WT; A24957) and *cdc14-3 GAL-cdc15(K54L)-3HA* (KD; A30371) cells were arrested in YEPRG at 37°C. Cdc15-3HA and cdc15-K54L-3HA were then immunopreciptated from these anaphase arrested cells as described previously (*9*) with the following modifications: 30 µl of anti-HA affinity matrix (Roche) were used, 3.5 mg of total protein were used per immunoprecipitation and kinase reactions incubated for 45 minutes. Substrate was 4 mg of either GST, GST-Nud1 (amino acids 1-150), or GST-nud1-S53A,S63A,T78A (amino acids 1-150).

GST fusion proteins were purified from *E. coli* in batch with glutathione-sepharose beads (Amersham). Kinase activity was measured using PhosphorImaging. The immunoblot signal was determined using ECL Plus (GE Healthcare) and fluorescence imaging. Quantifications were performed using NIH Image Quant software.

Dbf2 kinase assays

Dbf2 kinase assays were performed as in (*8*).

Immunoblot analysis

Antibody dilutions

Nud1-3V5 was detected using an anti-V5 antibody (Invitrogen) at a 1:2000 dilution. Cdc15-3HA, Mob1-6HA, and 3HA-Dbf2 were detected using an anti-HA antibody (HA.11, Covance) at a 1:2000 dilution. Mob1-eGFP and Cdc15-eGFP-Cnm67 (Cdc15-SPB) were detected using an anti-GFP antibody (Clontech, JL-8) at a 1:1000 dilution. Kar2 was detected using a rabbit anti-Kar2 antiserum (*10*) at a 1:200,000 dilution. Clb2 was detected using an anti-Clb2 antibody at a 1:2000 dilution (*11*). GST-Mob1 was detected with an α-GST-IRDye800 antibody and scanned with a LiCOR.

Phospho-immunoblots

To perform immunoblot analyses of Nud1 pT78, pS63, and pS53, Nud1-3V5 was immunoprecipitated under denaturing conditions as described previously (*12*). Nud1-3V5 was immunoprecipitated with anti-V5 agarose beads (Invitrogen). To test for Nud1 phosphorylation, blots were blocked in TBS-T plus 4.5% BSA for 4 hours and then incubated with the appropriate phospho-antibody in TBS-T plus 1% BSA (1:1000 dilution) overnight at 4°C. Blots were washed 5 times with TBS-T and then incubated with a goat anti-rabbit HRP secondary antibody (1:1000) in TBS-T plus 1% BSA for 1 hour at room temperature.

Antibody generation

Polyclonal antibodies to Nud1 pT78, pS63, and pS53 were raised against the peptides KPPTMTVLNNYSpTVHQKVPSGFC, PAISDpSVKKPC, and DFQDSNFTpSQVVEPAC, respectively. The antibodies were then affinity-purified using immobilized phosphopeptides (Abgent).

Peptide pull-down assays

Peptides used in pull-down experiments were N-terminally tagged with a long-chain biotin group (30.5 Å spacer) and C-terminally amidated. The sequences TVLNNYS-[T or pT]-VHQKVPS, FQDSNFT-[S or pS]-QVVEPAI, and VEPAISD-[S or pS]-VKKPPTM were used for the Nud1 T78, S53 and S63 sites, respectively. The sequences

LQSNVDD-[S or pSer]-VLRQKPD, YNTRRDT-[S or pSer]-TSTILFK, and RRDTSTS-[T or pThr]-ILFKPPV were used for the Hof1 S381, S517, and T520 sites, respectively. The peptide TVARIYH-[S or pSer]-VVRYAPS was used as the optimal binding peptide in these pull-down assays. The peptides (at ~1 mM) were bound to streptavidin beads (Pierce) in 10 mM Tris pH 8, 150 mM NaCl and washed twice with 9 mM Tris pH 8, 135 mM NaCl, 10% DMSO and three times with 10 mM Tris pH 8, 150 mM NaCl. Recombinant *MOB1* constructs (residues 79-314) were expressed as His_6-GST-tagged proteins in *E. coli* and purified on NiNTA beads (Qiagen). Purified proteins were bound to streptavidin beads (preloaded with peptides) at ~0.4 µg/µL in 10 mM Tris pH 8, 150 mM NaCl, 2 mM DTT and washed three times with 10 mM Tris pH 8, 150 mM NaCl, 2 mM DTT. Bound proteins were eluted by heating the beads in 6X sample loading buffer at 95°C and analyzed by SDS PAGE and Coomassie staining.

Peptide library screening

To explore the phospho-peptide binding activity of Mob1, we performed oriented peptide library screening using two synthetic phospho-peptide libraries to determine the optimal sequence for Mob1 binding. These libraries contain either a fixed phospho-threonine or phospho-serine flanked by four degenerate residue positions on each side. GST-Mob1 (aa79-314) was then incubated with the peptide libraries and the bound peptides eluted and sequenced (*13*). Mob1 selected for peptides containing specific amino acids N- and C-terminal to the orienting phospho-amino acid.

Peptide library screening was performed as described previously (*13*). In brief, ~0.5 mg of GST-Mob1 fusion protein was immobilized on glutathione beads and incubated with 1 mg of each oriented peptide library for 10 min at 4°C. Following extensive washing, the bound peptides were eluted using 30% acetic acid, dried in a Speed-Vac apparatus, resuspended in 80 µl of water, and sequenced by Edman degradation using an Applied Biosystems Model 477A protein sequencer. Selection ratios were calculated by comparing the mole-percentage of each amino acid in each position in the bound peptides compared to that in the starting library mixture. Values for the selected residues were then normalized to the mean values of the non-selected residues in each position.

The oriented peptide library screening revealed that Mob1 displayed a striking preference for Y or F in the -2 position and preferred aliphatic, hydrophobic, or R

residues in the +1 to +4 positions. Mob1 also appears to prefer phosphoserine over phosphothreonine, at least *in vitro* (Fig. 3D). Furthermore, the inclusion of positively charged amino acids C-terminal to the orienting phospho-amino acid led to less phospho-specific binding (Fig. 3D), the significance of which is at present unclear.

Fluorescence polarization measurements

Fluorescence polarization measurements were conducted with 5 nM FITC-labeled peptides and 0 to 100 µM Mob1 protein in 10 mM Tris pH 8, 0.15 M NaCl, 1 mM DTT, 0.05% Tween-20. FITC-AHA-TVLNNYS-pT-VHQKVPS and FITC-AHA-TVARIYH-pSer-VVRYAPS were used for the Nud1 pT78 and optimal peptides, respectively. The assays were performed in Corning 384-well black flat bottom plates with 40 µL per well. Each protein concentration was assayed in duplicate. Plates were read in a Tecan Group Infinite M1000 Pro plate reader. Each Kd was derived from a non-linear fit of all data points in the binding curve using the Prism software package.

Crystallography and structure determination

For the structural studies, amino acids 33-216 of human Mob1A were expressed from a modified pET28a vector containing a TEV-cleavable polyhistidine and GST tag in E. coli BL21 (DE3) cells. The recombinant protein was purified using GST-affinity purification (Glutathione Sepharose 4B, GE Healthcare), the purification tag removed using TEV protease and further purified using size exclusion chromatography (Superdex S75, GE Healthcare). The purified protein was concentrated to 8 mg/ml and mixed with a 1.2 molar excess of the synthetic phospho-peptide TVARIYHpSVVRYAPS in 150 mM NaCl, 20 mM Tris pH 8.0, 0.5 mM TCEP pH 8.0 and 1% (v/v) DMSO. Crystal screening was performed in MRC2 crystallization plates (Molecular Dimensions) using 0.2 µl sitting drops containing 50% protein and 50% well solution and commercial sparse crystallisation matrices (Hampton, Qiagen) at 18°C. Crystalline needles formed after 1-2 hours in 24% (w/v) PEG 6000 and 100 mM Tris pH 8.5. These needles were used to prepare a seed solution for microseeding experiments. Single crystals grew overnight in 22% (w/v) PEG3350, 100 mM Bicine pH 8.5 in drops containing 45% protein, 45% well solution, 5% protein buffer and 5% seed solution. For data collection, crystals were transferred into cryoprotectant solution containing mother liquor and protein buffer supplemented with 400mM phosphopeptide and 25% v/v glycerol, and flash-frozen in liquid nitrogen. Diffraction data were collected on an ADSC Q315r detector at 100 K on

beamline IO4 at the Diamond Light Source, Oxford, UK at a wavelength of 0.9795Å and processed using iMosflm (CCP4). The structure was solved by molecular replacement using PHASER (CCP4) with the human Mob1 structure (*14*) (PDB entry 1PI1) as the search model. Maps calculated using only protein phases revealed clear density for 8 residues of the peptide (YHpSVVRYA; Figure 4A) which were built into the model using Coot. Subsequent refinement was carried out using PHENIX. Relevant statistics are shown in Table S4. Coordinates have been deposited in the Protein Data Bank (PDBID:4JIZ).

The Mob1 structure revealed that the phosphopeptide binds across a shallow pocket on the Mob1 surface (Figs. 4A and S10) forming a beta-sheet with the linker region joining the 3rd and 4th major helical segments, somewhat reminiscent of the interaction of pTyr peptides with SH2 domains. Human and yeast Mob1 consistently select aromatic residues in the pSer/pThr -2 position and the basis for this is clear from our structure where the phenolic side-chain of Tyr -2 packs against the aliphatic portion of K84. In the highly homologous budding yeast Mob1, this lysine is substituted by a proline which would also make favorable van der Waals interactions. Indeed a similar structural mechanism is responsible for the selectivity of the BRCT domains from human Mdc1 for tyrosine at the +3 site (*15*)**.** Discrimination for small/medium hydrophobic residues at the +1 and +2 positions is also explained by their interactions with a largely conserved hydrophobic depression on the Mob1 surface. Most importantly, the structure nicely explains the phospho-dependence of Mob1 binding through extensive interactions of the phosphoserine with three basic residues (K132, R133, R136) that form part of a positively charged pocket located on the opposite face to the Dbf2-interacting surface. This pocket is conserved in the structures of *X. laevis* and *S. cerevisiae* Mob1 (*16, 17*). Intriguingly, a sulfate ion derived from the crystallization mother liquor lies bound within this basic pocket in the *S. cerevisiae* Mob1 structure (Fig. 4B). The presence of a sulfate ion in a basic pocket has previously been used to predict the location of a phosphopeptide binding domain (*13*). Three structurally equivalent arginine residues, R253, R254, and R257, form the conserved basic pocket of yeast Mob1 and directly coordinate the sulfate ion (Fig. 4B).

Cell cycle staging by spindle morphology

The stage of the cell cycle of individual cells was assessed by spindle morphology. G1 or S phase cells were defined as having unduplicated or newly duplicated spindle pole bodies but lacking a spindle that spanned the DAPI-stained nucleus. Metaphase cells were defined as cells with a thick, bar shaped spindles that spans an undivided DAPI-stained nucleus. Anaphase cells were defined as cells with separated DNA masses connected by an elongated spindle.

Circular dichroism

Mob1(amino acids 79-314) and mob1-3RA(amino acids 79-314) were expressed as His6-GST-fusions in *E. coli*, purified on NiNTA and GSH-agarose columns, followed by TEV cleavage and removal of the purification tags and TEV protease by a second passage through the GSH-agarose column and gel filtration. Protein solutions (300 µl samples at a concentration of 0.125 mg/ml in 10 mM Tris pH 8, 0.15M NaCl, 1 mM DTT) were loaded into a Starna Cells, Inc. quartz spectrophotometer cell (Catalog # 21-Q-1) and spectra were taken on an AVIV CD spectrophotometer Model 202. Scans were performed at room temperature from 250 nm to 195 nm in 1 nm steps with 5s averaging and 0.333s settling times.

Supplemental References

1. C. Janke *et al.*, *Yeast* **21**, 947 (2004).
2. M. S. Longtine *et al.*, *Yeast* **14**, 953 (1998).
3. U. Gruneberg *et al.*, *EMBO J* **19**, 6475 (2000).
4. R. D. Gietz, A. Sugino, *Gene* **74**, 527 (1988).
5. A. J. Bardin, A. Amon, *Nat Rev Mol Cell Biol* **2**, 815 (2001).
6. M. Geymonat, A. Spanos, G. de Bettignies, S. G. Sedgwick, *J Cell Biol* **187**, 497 (2009).
7. J. V. Kilmartin, A. E. Adams, *J Cell Biol* **98**, 922 (1984).
8. J. M. Rock, A. Amon, *Genes Dev* **25**, 1943 (2011).
9. S. L. Jaspersen, D. O. Morgan, *Curr Biol* **10**, 615 (2000).
10. M. D. Rose, L. M. Misra, J. P. Vogel, *Cell* **57**, 1211 (1989).
11. A. Amon, S. Irniger, K. Nasmyth, *Cell* **77**, 1037 (1994).
12. G. A. Brar *et al.*, *Nature* **441**, 532 (2006).
13. M. B. Yaffe *et al.*, *Cell* **91**, 961 (1997).
14. E. S. Stavridi *et al.*, *Structure* **11**, 1163 (2003).
15. M. Stucki *et al.*, *Cell* **123**, 1213 (2005).
16. S. Mrkobrada *et al.*, *J Mol Biol* **362**, 430 (2006).
17. L. Ponchon *et al.*, *Journal of molecular biology* **337**, 167 (2004).
18. J. M. Keck *et al.*, *Science* **332**, 1557 (2011).
19. X. Zhang *et al.*, *J Cell Sci* **122**, 2240 (2009).
20. H. Maekawa *et al.*, *J Cell Biol* **179**, 423 (2007).

21. C. J. Park *et al.*, *Eukaryot Cell* **7**, 444 (2008).
22. C. Konig, H. Maekawa, E. Schiebel, *J Cell Biol* **188**, 351 (2010).
23. F. C. Luca, M. Winey, *Mol Biol Cell* **9**, 29 (1998).
24. R. Visintin, A. Amon, *Mol Biol Cell* **12**, 2961 (2001).
25. F. Meitinger *et al.*, *Genes Dev* **25**, 875 (2011).
26. S. Ghaemmaghami *et al.*, *Nature* **425**, 737 (2003).

Acknowledgements

We thank Brian A. Joughin for assistance with molecular modeling during early phases of this work, Deborah Pheasant at the MIT Biophysical Instrumentation Facility for CD assistance, Matthew Webber for the use of the quartz cuvette, and the Koch Institute High Throughput Screening for the use of their plate reader.

Supplemental Figures

Fig. S1: Phosphorylation of the scaffold Nud1 is essential for MEN function.
(A) Schematic of Nud1 phosphorylation sites identified by mass spectrometry (*18*).

(B, C) *NUD1; NUD1-3V5* (A27463) and *NUD1; nud1-42A-3V*5 (A29128) cells were arrested in G1 with α-factor pheromone (5 µg/ml) in YEP medium containing glucose (YEPD). When the arrest was complete (after 150 min), cells were released into pheromone free YEPD medium. After 80 minutes, α-factor (10 µg/ml) was re-added to prevent entry into the subsequent cell cycle. The percentage of cells with metaphase (black closed squares, B) and anaphase spindles (red closed circles, B) was determined at the indicated times. Nud1-3V5 and nud1-42A-3V5 protein levels were monitored by Western blot analysis (C). Kar2 was used as a loading control.
Note the residual phosphorylation of the nud1-42A protein could be due to phosphorylation of sites not covered by the mass spectrometry analysis and/or alternative site usage by Nud1 kinases. The fact that nud1-42A is present at wild-type levels, is a substrate for mitotic kinases, and localizes to SPBs indicates that the overall folding and structure of the protein are not grossly affected by the alanine substitutions.

(D) *NUD1; NUD1-3V5* (A27463), *NUD1; nud1-42A-3V5* (A29128), or no tag control (A2587) cells were grown to exponential phase to examine Nud1 (α-V5) and α-tubulin

localization in anaphase cells. 4′6-diamidino-2-phenylindole (DAPI) was used to stain DNA.

(E) Wild-type (A2587), *GAL-nud1-44* (A29248), *GAL-nud1-44; NUD1-3V5* (A29685), and *GAL-nud1-44; nud1-42A-3V5* (A29500) cells were spotted on YEP plates containing either galactose and raffinose (YEPRG) or glucose (YEPD) and incubated at room temperature (YEPRG) or 37°C (YEPD). Approximately 3 X 10^4 cells were deposited in the first spot and each subsequent spot is a 10-fold serial dilution. The pictures shown depict 1.5 days of growth (YEPD) or 3 days of growth (YEPRG).

(F) *GAL-nud1-44; NUD1-3V5* (A29878) and *GAL-nud1-44; nud1-42A-3V5* (A29881) cells containing a 3HA-Cdc14 fusion protein were grown for 2 hours in YEP medium containing glucose at 37°C to examine Cdc14 (α-HA) and α-tubulin localization. Cells were scored as having either correctly positioned (anaphase spindle aligned along the mother-daughter cell axis) or mis-positioned anaphase spindles, the presence or absence of detached astral microtubules, and released or sequestered Cdc14. The white arrowhead marks a detached astral microtubule.

Fig. S2: MEN component localization in *nud1-42A* mutants.
Why it was necessary to introduce the DBF2-HyA and SPC72-CNM67 alleles into the strains used in in Fig. S2 is explained in the Materials and Methods section entitled "NUD1 phospho-mutant allele analysis."

(A) Exponentially growing *nud1Δ; NUD1-3V5 DBF2-HyA SPC72-CNM67* (A29412) and *nud1Δ; nud1-42A-3V5 DBF2-HyA SPC72-CNM67* (A29508) cells were prepared for immunofluorescence with anti-V5 antibodies (α-V5) and anti-tubulin antibodies (α-tubulin) to examine Nud1 and tubulin localization, respectively. 4′6-diamidino-2-phenylindole (DAPI) was used to stain DNA. Cell cycle stage was determined based on spindle morphology and correlated with Nud1 localization at SPBs ($n \geq 100$ cells). Representative images of anaphase cells are shown.

(B) *NUD1-3V5 DBF2-HyA SPC72-CNM67 BFA1-eGFP* (A29733) and *nud1-42A-3V5 Dbf2-HyA SPC72-CNM67 BFA1-eGFP* (A29730) cells containing an mCherry-Tub1 fusion protein were grown to log phase in SC-Leu medium and imaged after a brief

paraformaldehyde fixation. 4′6-diamidino-2-phenylindole (DAPI) was used to stain DNA. Cell cycle stage was determined based on spindle morphology and correlated with Bfa1 localization at SPBs (n ≥ 100 cells). Representative images of anaphase cells are shown.

(C) *NUD1-3V5 DBF2-HyA SPC72-CNM67 TEM1-GFP* (A29899) and *nud1-42A-3V5 Dbf2-HyA SPC72-CNM67 TEM1-GFP* (A29679) cells containing a mCherry-Tub1 fusion protein were grown and scored as in Fig. S2B. Representative images of anaphase cells are shown.

(D) *NUD1-3V5 DBF2-HyA SPC72-CNM67 CDC15-eGFP* (A28650) and *nud1-42A-3V5 DBF2-HyA SPC72-CNM67 CDC15-eGFP* (A29506) cells containing a mCherry-Tub1 fusion protein were grown and scored as in Fig. S2B. Representative images of anaphase cells are shown.

(E) *NUD1-3V5 DBF2-HyA SPC72-CNM67 MOB1-eGFP* (A29450) and *nud1-42A-3V5 DBF2-HyA SPC72-CNM67 MOB1-eGFP* (A29722) cells containing a mCherry-Tub1 fusion protein were grown and scored as in Fig. S2B. Representative images of anaphase cells are shown.

(F) *NUD1-3V5 DBF2-HyA SPC72-CNM67 DBF2-eGFP* (A29711) and *nud1-42A-3V5 DBF2-HyA SPC72-CNM67 DBF2-eGFP* (A29682) cells containing an mCherry-Tub1 fusion protein were grown to log phase in SC-Leu medium and imaged and scored as in Fig. S2B. Representative images of anaphase cells are shown.

Fig. S3: Identification of the Nud1 phosphorylation sites necessary for Dbf2-Mob1 localization to SPBs and MEN function.
To define the phosphorylation sites required for Dbf2-Mob1 recruitment to SPBs we took advantage of the fact that overexpression of the nud1-42A allele causes lethality and arrests cells in anaphase with Cdc14 sequestered in the nucleolus. We created NUD1 alleles harboring a subset of phosphorylation site mutations and identified critical residues by virtue of whether or not they cause lethality when overexpressed.

(A) Wild-type (A2587), *NUD1; GAL-NUD1-3V5* (A27931), *NUD1; GAL-nud1-42A-3V5* (A29239), *NUD1; GAL-nud1-27A-3V5* (A27933), *NUD1; GAL-nud1-20A-3V5* (A30611),

NUD1; GAL-nud1-16A-3V5 (A30614), *NUD1; GAL-nud1-12A-3V5* (A30617), *NUD1; GAL-nud1-8A-3V5* (A30620), *NUD1; GAL-nud1-7A-3V5* (A30623), *NUD1; GAL-nud1-6A-3V5* (A30649), *NUD1; GAL-nud1-4A-3V5* (A30652), and *NUD1; GAL-nud1-S53A S63A T78A-3V5* (A30652) cells were spotted on YEPRG or YEPD plates as in Fig. S1E. The cartoon on the left shows the mutations contained in each *nud1* phospho-mutant allele.

(B) Wild-type (A2587), *NUD1; GAL-NUD1-3V5* (A27931), *NUD1; GAL-nud1-27A-3V5* (A27933), *NUD1; GAL-nud1-25A-3V5* (A30917), *NUD1; GAL-nud1-24A-3V5* (A30915), *NUD1; GAL-nud1-23A-3V5* (A31176), and *NUD1; GAL-nud1-21A-3V5* (A30913) cells were spotted on YEPRG or YEPD plates as in Fig. S1E. The cartoon on the left shows the mutations contained in each *nud1* phospho-mutant allele.

(C) Wild-type (A2587), *NUD1; GAL-NUD1-3V5* (A27931), *NUD1; GAL-nud1-42A-3V5* (A29239), *NUD1; GAL-nud1-S49A S53A S63A-3V5* (A30655), *NUD1; GAL-nud1-T78A-3V5* (A30925), *NUD1; GAL-nud1-S53A T78A-3V5* (A31209), *NUD1; GAL-nud1-S63A T78A-3V5* (A31211), and *NUD1; GAL-nud1-S53A S63A T78A-3V5* (A31215) cells were grown to exponential phase in YEP medium containing raffinose. Galactose was added a t = 0 to induce the *GAL1-10* promoter. The percentage of cells with anaphase spindles was determined at the indicated times using spindle morphology as a criterion.

(D) Wild-type (A2587), *nud1Δ GAL-nud1-44* (A29248), *nud1Δ GAL-nud1-44 NUD1-3V5* (A29685), *nud1Δ GAL-nud1-44 nud1-42A -3V5* (A29500), and *nud1Δ GAL-nud1-44 nud1(3A)-3V5* (A32292) cells were spotted on YEPRG or YEPD plates as in Fig. S1E. *It should further be noted that the nud1-3A and nud1-42A alleles cannot support proliferation when present as the sole NUD1 allele. Cells harboring these nud1 alleles as the sole source of NUD1 cannot be recovered from crosses.*

Fig. S4: Conservation of the Nud1 phosphorylation sites.
(A) Regional evolutionary constraints for Nud1 were calculated in (*18*). The *Y* axis represents the Nud1 regional evolutionary constraint value among fungi (17 amino acid sliding regions) where a value of 1 indicates full conservation across all orthologs; the *X* axis depicts the amino acid position of Nud1. Green dots and red dots represent

identified phosphorylation sites in Nud1 (the red dots mark S53, S63, and T78). Adapted from (*18*).

(B) Positional evolutionary constraints for Nud1 were calculated in (*18*). The *Y* axis is the Nud1 positional evolutionary constraint value among fungi where a value of 1 indicates full conservation across all orthologs; the *X* axis is the amino acid position of Nud1. Dashed lines indicate the average Nud1 positional evolutionary constraint value (avg) and 1 standard deviation above this value (1σ). Highlighted in red are amino acids S53, S63, and T78. Adapted from (*18*).

(C) BLASTP was used to identify the five closest fungal homologs of the N-terminus of Nud1 (amino acids 1 – 400). These homologs were aligned with Nud1 using ClustalW2. Nud1 S53, S63, and T78 are highlighted in red.

Fig. S5: Nud1 phosphorylation is required for anaphase astral microtubule anchorage and spindle positioning.
(A) Wild-type (A2587), *GAL-nud1-44; NUD1-3V5* (A29685), *GAL-nud1-44; nud1-42A-3V5* (A29500), *GAL-nud1-44; nud1-3A-3V5* (A32293), and *GAL-nud1-44; nud1-39A-3V5* (A32295) cells were grown for 2 hours in YEP medium containing glucose at 37°C to examine spindle morphology. Cells were scored as having either correctly positioned (anaphase spindle aligned along the mother-daughter cell axis) or mis-positioned anaphase spindles. Whether or not astral microtubules were detached was also assessed. The white arrowheads mark detached astral microtubules.

(B) Wild-type *NUD1* (A32731) and *nud1-39A-3V5* (A32730) cells containing GFP-Tub1 and SV40NLS-mCherry fusions were grown to log phase in complete synthetic medium and analyzed by live cell microscopy. The time to exit from mitosis was defined as the time interval between entry of the daughter-bound SPB into the bud and breakdown of the anaphase spindle ($n \geq 30$ cells). Data are summarized in box-and-whisker plots: boxes span the 25th and 75th percentile with a line at the median; whiskers extend from the minimum value to the maximum. *$p < 0.05$, t test.

(C) *nud1Δ; NUD1-3V5* (A32241) and *nud1Δ; nud1(39A)-3V5* (A31472) cells containing a GFP-Tub1 fusion protein were grown to log phase in YEPD medium and imaged after a

brief paraformaldehyde fixation. Cells were scored as in Fig. S5A. Representative images of anaphase cells are shown. The white arrowheads mark detached astral microtubules.

(D) Wild-type (A32731) and *nud1-39A-3V5* (A32730) cells containing a GFP-Tub1 and SV40NLS-mCherry fusions were grown to log phase in complete synthetic medium and analyzed by live cell microscopy. Representative montages of a wild-type cell with a correctly positioned anaphase spindle (top row), a *nud1-39A-3V5* cell with a correctly positioned anaphase spindle (middle row), and a *nud1-39A-3V5* cell with a mis-positioned anaphase spindle (bottom row) are shown. The white arrowheads mark detached astral microtubules.
The live-cell microscopy revealed that detachment of astral microtubules occurred during anaphase. The majority (80%) of metaphase nud1-39A cells showed proper nuclear migration and spindle alignment and underwent a normal anaphase (regardless of the presence of detached astral microtubules). However, 20% of metaphase nud1-39A cells failed to properly position the nucleus and subsequently underwent anaphase in the mother cell with a mispositioned spindle. The majority of these cells arrested in anaphase for approximately 3 hours, after which they exited mitosis. The anaphase-specific spindle alignment defect suggests that dynein-dependent spindle positioning is defective in nud1-39A cells. Consistent with this idea, we found that deleting DYN1 did not interfere with proliferation of nud1-39A cells, but deleting KAR9 did.

(E) *nud1Δ; NUD1-3V5* (A32241), *SPC72-CNM67* (A32796), *nud1Δ; nud1-39A-3V5* (A31472), and *nud1Δ; nud1-39A-3V SPC72-CNM67 5* (A32793) cells containing a GFP-Tub1 fusion were grown to log phase in YEPD medium and imaged. Cells were scored as in Fig. S5A.

(F) Wild-type (A27353) and *nud1-39A-3V5* (A31466) cells containing an *SPC72-eGFP* fusion protein were grown to log phase in YEPD medium and imaged after a brief paraformaldehyde fixation. Quantified relative fluorescent intensities in G1 and early S phase cells and anaphase cells are shown as box-and-whisker plots. Boxes span between the 25^{th} and 75^{th} percentile with a line at the median; whiskers extend from the minimum value to the maximum. n.s. = not significant, ***$p < 0.001$, t test.

The data show that the phosphorylation of Nud1 in mitosis is required for targeting the γ–tubulin complex binding protein Spc72 to Nud1, which in turn is necessary for the anchoring of astral microtubules to SPBs and proper positioning of the anaphase spindle. In higher eukaryotes, Polo kinase plays an essential role in localizing the γ–tubulin complex to centrosomes (19). As Cdc5 phosphorylates Nud1 (20, 21), Cdc5 may play a conserved role in the phosphorylation of a centrosome/SPB-localized scaffold to promote the recruitment of the γ–tubulin complex.

Fig. S6: Cdc15 kinase activity is necessary for localization of Dbf2-Mob1 to SPBs
CDC15-eGFP MOB1-mCherry (A31089) and *cdc15-as1-eGFP MOB1-mCherry* (A31355) cells were grown for 2 hours in YEPD supplemented with 10 µM 1-NA-PP1. Cells were imaged after a brief paraformaldehyde fixation and Cdc15 and Mob1 localization was analyzed in anaphase cells (n ≥ 100 cells).
The results show that in cells carrying the analog sensitive cdc15-as1 allele grown in the presence of inhibitor Dbf2-Mob1 cannot localize to SPBs (22). Importantly, treatment of cdc15-as1 cells with inhibitor arrested cells in anaphase with Cdc15 localized to both SPBs, thus Cdc15 kinase activity at SPBs, and not simply Cdc15 protein, is necessary for Dbf2-Mob1 SPB localization. These findings are consistent with previous data showing that Dbf2-Mob1 cannot localize to SPBs in cdc15-2 cells (23, 24).

Fig. S7: Targeting Cdc15 to SPBs induces Nud1 phosphorylation.
NUD1-3V5 (A24513) and *NUD1-3V5 MET3-CDC15-SPB* (A31422) cells were arrested in G1 with α factor (5 µg/ml), S phase with hydroxyurea (200 mM), or metaphase with nocodazole (15 µg/ml) in YEPD supplemented with 8 mM methionine. When the arrest was complete (after 2 hours), cells were transferred into CSM-methionine medium containing glucose and α factor, hydroxyurea, or nocodazole to induce Cdc15-SPB expression. Nud1-3V5, Cdc15-SPB, Clb2, and Kar2 levels were monitored by Western blotting at the indicated time points.
The data show that expression of CDC15-SPB induces premature Nud1 phosphorylation. Upon induction of CDC15-SPB expression slower migrating phospho-forms of Nud1 became apparent in G1, S phase or metaphase-arrested cells. The Cdc15-SPB-dependent shift in Nud1 mobility was not the result of the cells escaping the cell cycle block as levels of the mitotic cyclin Clb2 did not change significantly upon CDC15-SPB induction.

Fig. S8: Nud1 phospho-antibodies are phospho-specific.

*nud1*Δ; *NUD1-3V5 cdc14-3 DBF2-HyA* (A32483) and *nud1*Δ; *nud1-S53A,S63A,T78A-3V5 cdc14-3 DBF2-HyA* (A32507) cells were grown to log phase in SC-Leu medium at room temperature and then arrested in anaphase by shifting cells to 37°C for 2 hours. Nud1-3V5 and nud1-S53A S63A T78A-3V5 were immunoprecipitated under denaturing conditions and phosphorylation of Nud1 T78 (α-pT78; A), S63(α -pS63; B), S53(α -pS53; C), and total Nud1 (a-V5) were examined by Western blot analysis.

Fig. S9: Oriented peptide library screening of Mob1 and Mob1 – phosphopeptide binding affinities.

(A, B) Mob1 binding specificities identified using the phospho-threonine and phospho-serine oriented degenerate peptide libraries. GST-Mob1 (aa79-314) was screened with peptide libraries containing the sequence MAXXXXpTXXXXAKKK or MAXXXXXpSXXXXXAKKK where X indicates all amino acids except Cys. Enrichment values, shown in parentheses, indicate a quantitative measure of the preference of Mob1 for that particular amino acid at that particular position. A value of 1 indicates neither preference nor discrimination, values of 1.3 or greater indicate moderate selection, and values of 1.7 or greater indicate strong selection. Amino acids are denoted in single letter code.

(C) Sequence context of Nud1 S53, S63, and T78. Highlighted in yellow are residues that conform to the Mob1 sequence preferences identified in the oriented peptide library screening.

(D) Phosphorylated (p-optimal, pT78) or non-phosphorylated (optimal, T78) peptides bound to Streptavidin beads were incubated with GST-Mob1(aa79-314). The amount of GST-Mob1 bound to beads and input were analyzed by Coomassie staining. The optimal peptide sequence is based on the peptide library screening and is TVARIYH-pSer or Ser-VVRYAPS; the pT78/T78 peptide sequence is derived from Nud1 and is TVLNNYS-pThr or Thr-VHQKVPS.

(E) The dissociation constants of the Mob1-optimal phospho-peptide and the Nud1 pT78 peptide complexes were determined by fluorescence polarization measurements.

Figure S10: The Mob1-bound phosphopeptide is well defined in the co-crystal structure.

(A) SIGMAA-weighted 2Fo-Fc electron density omit map for the phospho-peptide overlayed upon the final refined peptide coordinates in a stick-representation. Residues are numbered from -2 to +5 with respect to the central pSer. The map is contoured at 1.5σ.

(B) Sequence comparison of the residues surrounding *S. cerevisiae* Mob1 R253-R257 with this Mob1 region from other species.

Fig. S11: The mob1-3RA protein is properly folded but defective in *MOB1* function.

(A) Mob1(aa79-314) and mob1-3RA(aa79-314) were purified to homogeneity and analyzed by circular dichroism. Consistent with what is seen in the crystal structure, the 208 and 222 nm dips confirm that these proteins are largely alpha-helical.

(B) A3911, A31548, A31728, A31730, A31732, A31550, A31502, A31901, A31905, A31909, and A31506 cells were grown to log phase in YEPD. Dbf2-3HA was immunoprecipitated and bound Mob1 (IP α-GFP), bound Dbf2 (IP α-HA), total Mob1 (input α-GFP), and total Dbf2 (input α-HA) were monitored by Western blot analysis.

(C) A31500, A31893, A31895, and A31897 cells were grown to log phase in YEPD and imaged after a brief paraformaldehyde fixation. Mob1 localization was analyzed in anaphase cells.

(D) A2587, A32452, A32586, A32592, A32595, A32598, and A32589 cells were spotted on YEPRG or YEPD plates and incubated at room temperature (YEPRG) or 37°C (YEPD) as in Fig. S1E.

(E) Wild-type (A32979), *DBF2-HyA* (A28022), *GAL-mob1-77* (A32986), *DBF2-HyA GAL-mob1-77* (A32551), *MOB1-eGFP; GAL-mob1-77* (A32988), *DBF2-HyA MOB1-eGFP; GAL-mob1-77* (A32674), *mob1-R253A R254A R257A-eGFP; GAL-mob1-77* (*3RA*, A32990), and *DBF2-HyA mob1-R253A R254A R257A-eGFP; GAL-mob1-77* (*3RA*, A32676) cells were spotted on SC-Leu plates containing raffinose and galactose (SC-

LeuRG) or SC-Leu plates containing glucose (SC-Leu) and incubated at room temperature (SC-LeuRG) and 37°C (SC-Leu). Approximately $3x10^4$ cells were deposited in the first spot and each subsequent spot is a 10-fold serial dilution.

Fig. S12: Mob1 interacts with Hof1 phosphopeptides.
Phosphorylated (pS381, pS517, pT520) or non-phosphorylated (S381, S517, T520) Hof1 peptides bound to Streptavidin beads were incubated with GST-Mob1. Input and the amount of Mob1 bound to beads were analyzed by Coomassie staining.
The results show that the phosphopeptide binding property of Mob1 is not only critical for targeting Dbf2-Mob1 to SPBs for activation, but also for targeting Dbf2-Mob1 to its substrates. Previous studies showed that Cdc5 phosphorylates the F-BAR protein Hof1 to facilitate Hof1-Mob1 binding and subsequent Hof1 phosphorylation by Dbf2 (25). Our data show that Mob1 can bind phosphopeptides derived from experimentally verified Cdc5-dependent Hof1 phosphorylation sites. We propose that at least some Dbf2-Mob1 substrates require phosphorylation by a priming kinase in order to be recognized and phosphorylated by Dbf2-Mob1.

Fig. S13: The overexpression of MEN components does not affect the kinetics of Cdc14 release from the nucleolus and exit from mitosis.
Overexpression of either *TEM1, CDC15, DBF2, MOB1* or *NUD1* does not affect the kinetics of Cdc14 release from the nucleolus and exit from mitosis. Wild-type (A2587), *GAL-TEM1* (A2441), *GAL-CDC15* (A4084), *GAL-DBF2* (A2546), *GAL-MOB1* (A32612), and *GAL-NUD1* (A27931) cells were arrested in G1 with α-factor pheromone (5 µg/ml) in YEP medium containing raffinose (YEPRaff). One hour prior to release, galactose was added (2% final concentration) to induce expression of the *GAL1-10* promoter. When arrest complete (after 170 minutes), cells were released into pheromone free YEPRaffGal medium. After 80 minutes, α-factor (10 µg/ml) was re-added to prevent entry into the subsequent cell cycle. The percentage of cells with metaphase (closed squares) and anaphase (open circles) spindles and Cdc14 release from the nucleolus (closed circles) was determined at the indicated times.

Fig. S14: The interaction between Dbf2-Mob1 and Nud1 must be dynamic.
Note: expression of the MOB1-eGFP-NUD1 fusion protein from the endogenous MOB1 promoter is lethal so we placed the MOB1-NUD1 fusion under the control of the low-

strength methionine repressible MET3 promoter. We will refer to the fusion as the MOB1-NUD1 fusion.

(A) *MOB-NUD1 SPC42-mCherry* (A32624) cells were grown to log phase in YEPD supplemented with 8 mM methioinine. Cells were then shifted to CSM medium lacking methionine and containing glucose for 60 minutes to induce expression of the *MOB1-NUD1* fusion and imaged after a brief paraformaldehyde fixation. Representative images of G1/S, metaphase, and anaphase cells are shown.

(B) *MOB1-NUD1 DBF2-tdTomato* (A32797) cells were grown to log phase in YEPD supplemented with 8 mM methioinine. Cells were then shifted to CSM medium lacking methionine and containing glucose for 60 minutes to induce expression of the *MOB1-NUD1* fusion and imaged after a brief paraformaldehyde fixation. Representative images of G1/S, metaphase, and anaphase cells are shown.

(C) Wild-type (A2587), *mob1-77* (A31479), *MOB1-NUD1* (A32336), and *MOB1-NUD1 mob1-77* (A32635) cells were spotted on YEPD plates supplemented with 8 mM methioinine and incubated at 30°C or 37°C.

(D) Wild-type (A2587) and *MOB1-NUD1* (A32336) cells were spotted on YEPD plates supplemented with 8 mM methionine or CSM medium lacking methionine and containing glucose and incubated at 30°C.

(E) Wild-type (A2747) and *MOB1-NUD1* (A32667) cells were arrested in G1 with α-factor pheromone (5 µg/ml) in YEPD medium. One hour prior to release, cells were shifted to CSM medium lacking methionine and containing glucose supplemented with α-factor pheromone (5 µg/ml) to induce expression of the *MOB1-NUD1* fusion. When the arrest was complete (after 170 minutes), cells were released into pheromone free CSM medium lacking methionine and containing glucose. After 70 minutes, α-factor pheromone (10 µg/ml) was re-added to prevent entry into the subsequent cell cycle. The percentage of cells with metaphase spindles (black closed squares), anaphase spindles (red closed circles), and 3HA-Cdc14 released from the nucleolus (open circles) was determined at the indicated times.

(F) Wild-type (A2587), *TAB6-1* (A28436), *MOB1-NUD1* (A32336), and *MOB1-NUD1 TAB6-1* (A32661) cells were spotted on YEPD plates supplemented with 8 mM methionine or CSM medium lacking methionine and containing glucose and incubated at 30°C.

(G) Wild-type (A32979), *DBF2-HyA* (A28022), *GAL-mob1-77* (A32986), *GAL-mob1-77 DBF2-HyA* (A32551), *MOB1-NUD1 GAL-mob1-77* (A32992), and *MOB1-NUD1 GAL-mob1-77 DBF2-HyA* (A32881) cells were spotted on SC-Leu plates containing raffinose, galactose, and methionine (SC-LeuRG+Met. RT) or CSM medium lacking methionine and containing glucose (CSM-Met. 37°C) and incubated at room temperature (SC-LeuRG+Met. RT) or 37°C (CSM-Met. 37°C).

Note: attempts to determine whether the Dbf2-Mob1 fusion harbored kinase activity were unsuccessful, presumably because the Mob1-Nud1 protein is tightly bound to the SPB and thus is not amenable to standard Dbf2 IP-kinase assays. However, it is interesting to note that the anaphase arrest of MOB1-NUD1 cells was not suppressed by a constitutively active Dbf2 allele (DBF2-HyA), arguing that even constitutively active Dbf2-Mob1, when not able to dissociate from Nud1, cannot promote exit from mitosis (G). Furthermore, the dynamic association of Dbf2-Mob1 with SPBs could provide a means of signal amplification. Dbf2 and Mob1 are present at 15 – 21 fold higher concentrations in vivo than their activator Cdc15 (26). Thus, the dynamic association of Dbf2-Mob1 with Nud1 allows few molecules of Cdc15 to activate many molecules of Dbf2-Mob1.

Figure S1

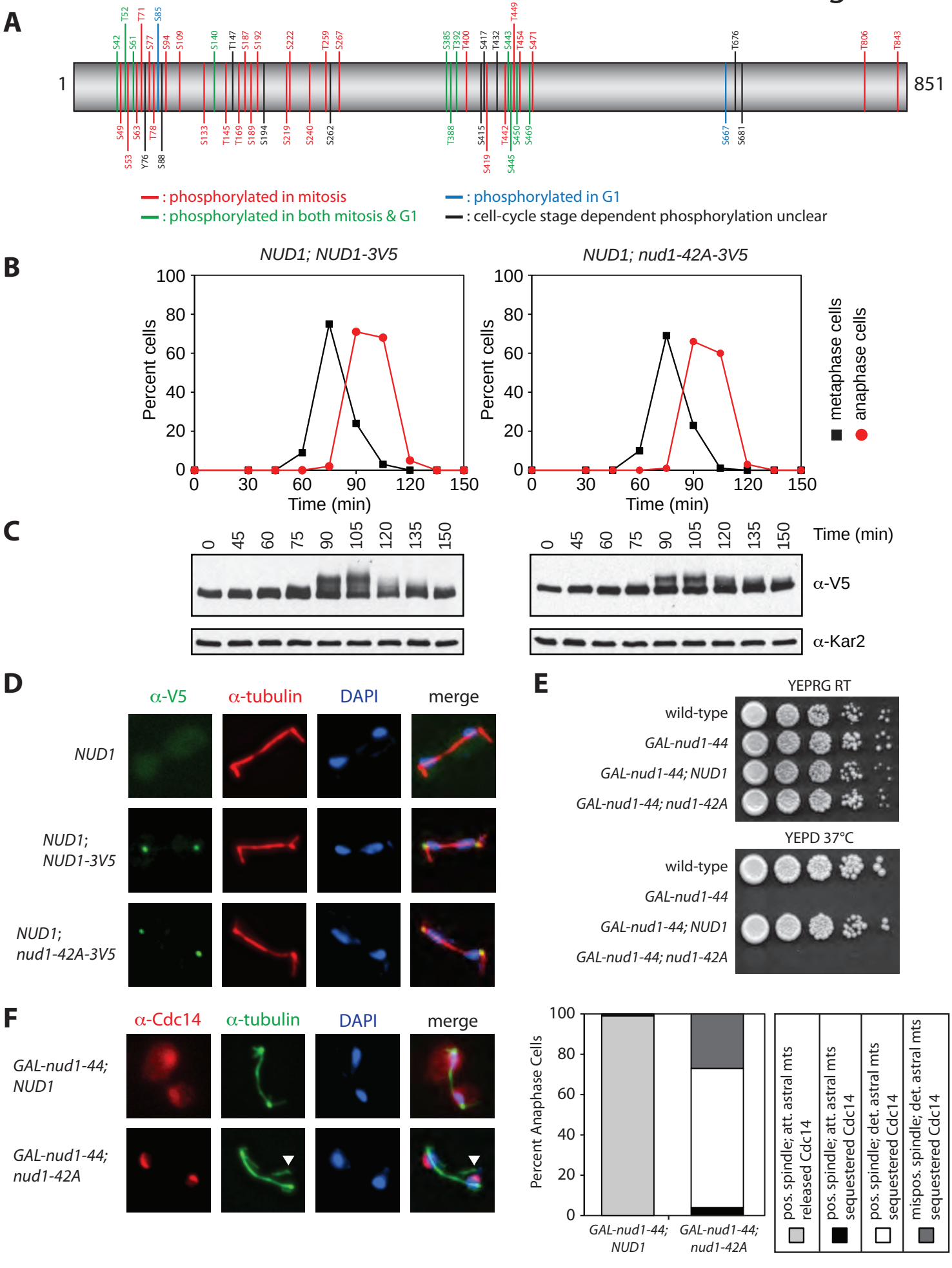
A
1
851
S42 T52 S61 T71 S77 S85 S94 S109 S140 T147 S187 S192 S222 T259 S267 S385 T392 T400 S417 T432 S443 T449 T454 S471 T676 T806 T843
S49 S53 S63 Y76 T78 S88 S133 T145 T169 S189 S194 S219 S240 S262 T388 S415 S419 T442 S445 S450 S469 S667 S681
: phosphorylated in mitosis
: phosphorylated in both mitosis & G1
: phosphorylated in G1
: cell-cycle stage dependent phosphorylation unclear
B
NUD1; NUD1-3V5
NUD1; nud1-42A-3V5
Percent cells
Time (min)
metaphase cells
anaphase cells
C
Time (min)
α-V5
α-Kar2
D
α-V5
α-tubulin
DAPI
merge
NUD1
NUD1; NUD1-3V5
NUD1; nud1-42A-3V5
E
YEPRG RT
YEPD 37°C
wild-type
GAL-nud1-44
GAL-nud1-44; NUD1
GAL-nud1-44; nud1-42A
F
α-Cdc14
α-tubulin
DAPI
merge
GAL-nud1-44; NUD1
GAL-nud1-44; nud1-42A
Percent Anaphase Cells
pos. spindle; att. astral mts released Cdc14
pos. spindle; att. astral mts sequestered Cdc14
pos. spindle; det. astral mts sequestered Cdc14
mispos. spindle; det. astral mts sequestered Cdc14

Figure S2

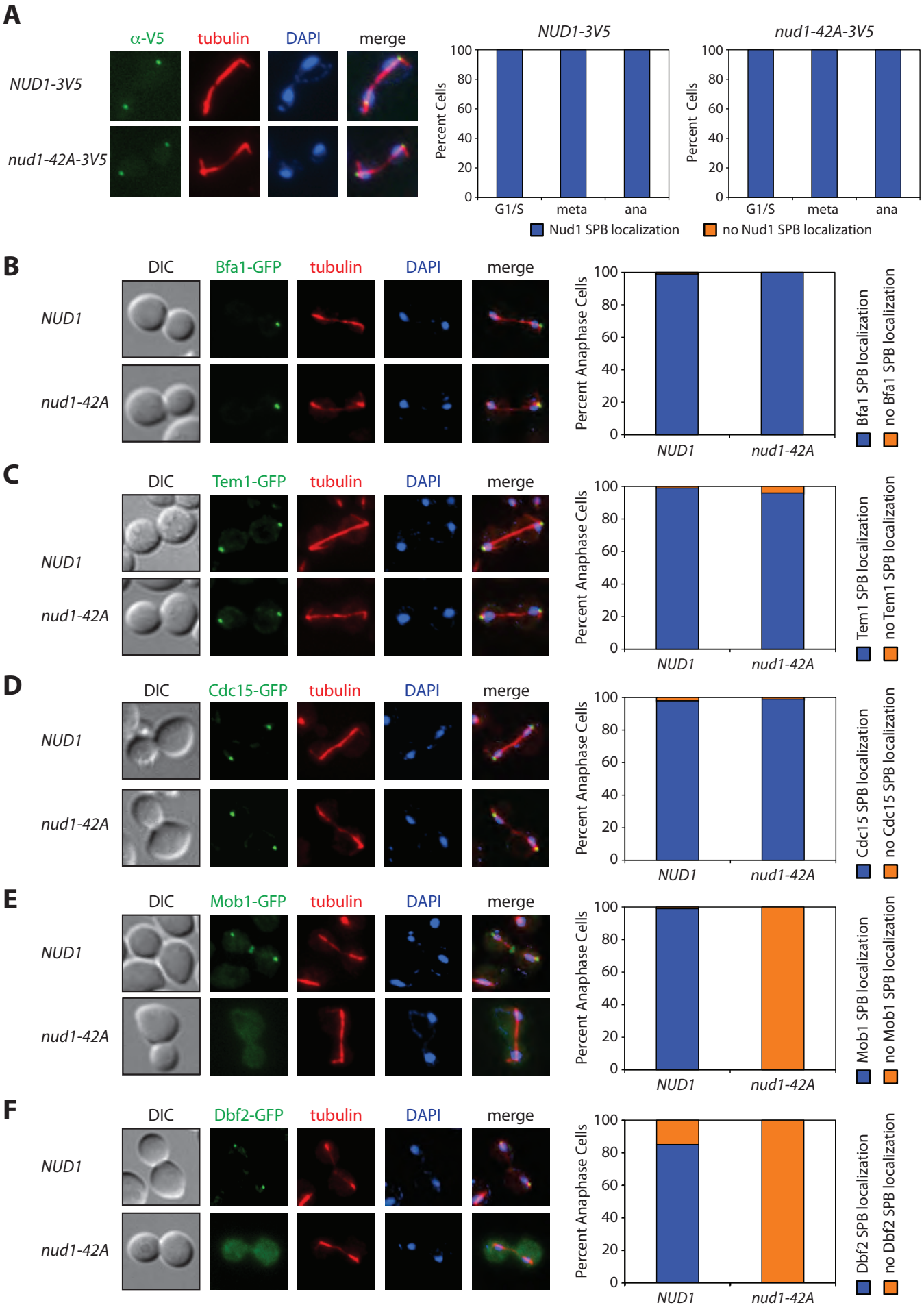
A
α-V5
tubulin
DAPI
merge
NUD1-3V5
nud1-42A-3V5
NUD1-3V5
nud1-42A-3V5
Percent Cells
100
80
60
40
20
0
G1/S
meta
ana
Nud1 SPB localization
no Nud1 SPB localization
B
DIC
Bfa1-GFP
tubulin
DAPI
merge
NUD1
nud1-42A
Percent Anaphase Cells
Bfa1 SPB localization
no Bfa1 SPB localization
C
DIC
Tem1-GFP
tubulin
DAPI
merge
NUD1
nud1-42A
Percent Anaphase Cells
Tem1 SPB localization
no Tem1 SPB localization
D
DIC
Cdc15-GFP
tubulin
DAPI
merge
NUD1
nud1-42A
Percent Anaphase Cells
Cdc15 SPB localization
no Cdc15 SPB localization
E
DIC
Mob1-GFP
tubulin
DAPI
merge
NUD1
nud1-42A
Percent Anaphase Cells
Mob1 SPB localization
no Mob1 SPB localization
F
DIC
Dbf2-GFP
tubulin
DAPI
merge
NUD1
nud1-42A
Percent Anaphase Cells
Dbf2 SPB localization
no Dbf2 SPB localization

Figue S3

A

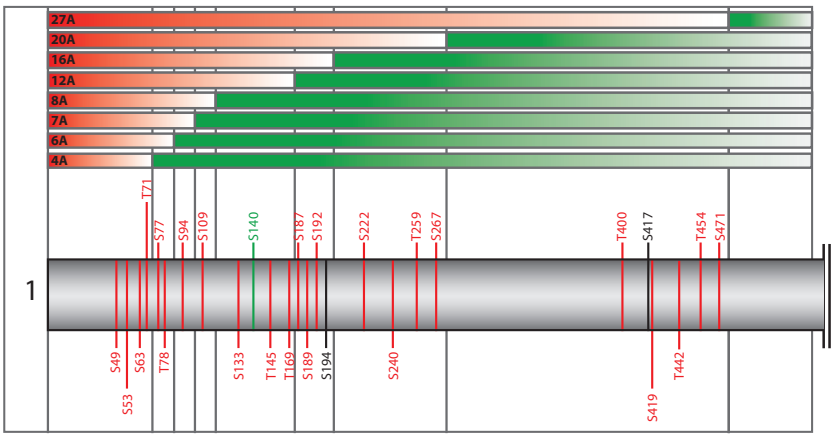

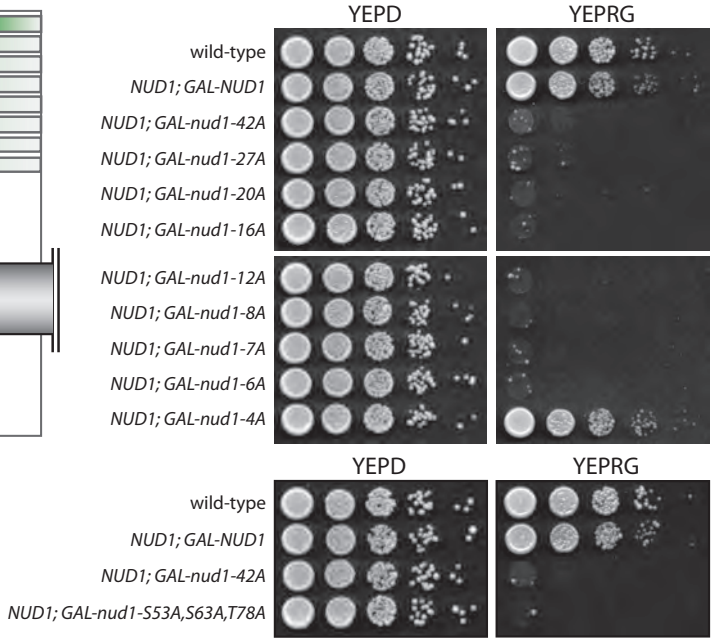

B

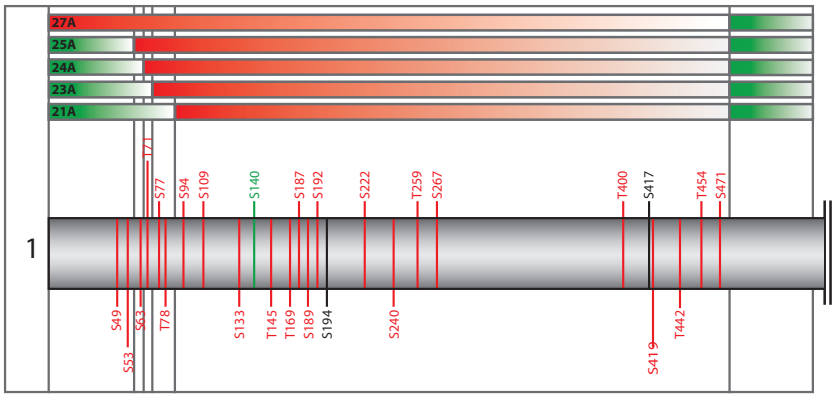

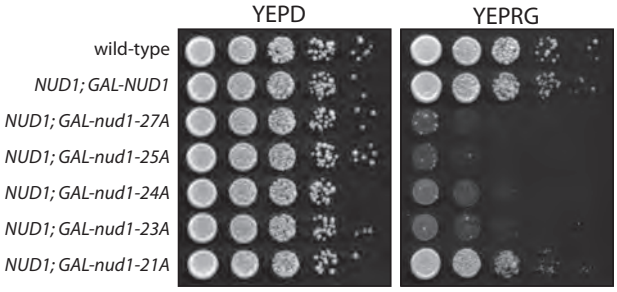

C

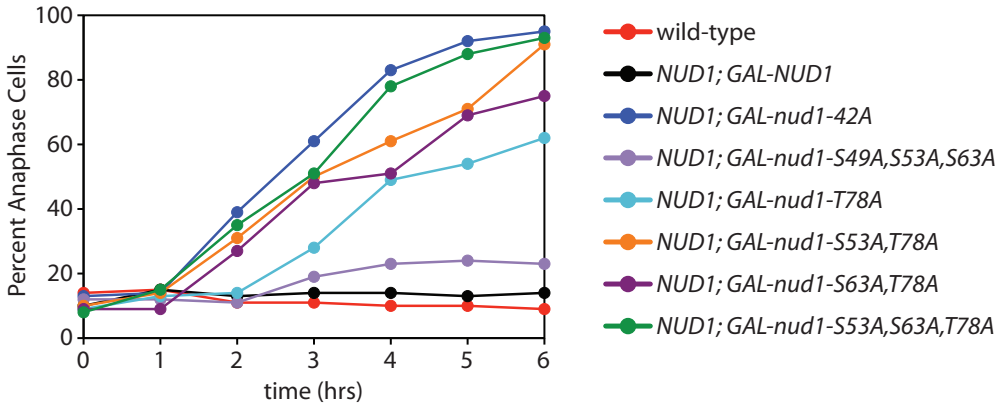

D

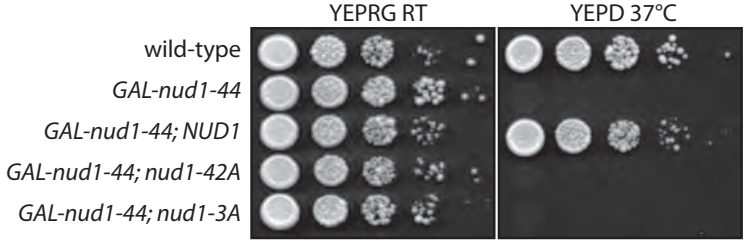

Figure S4

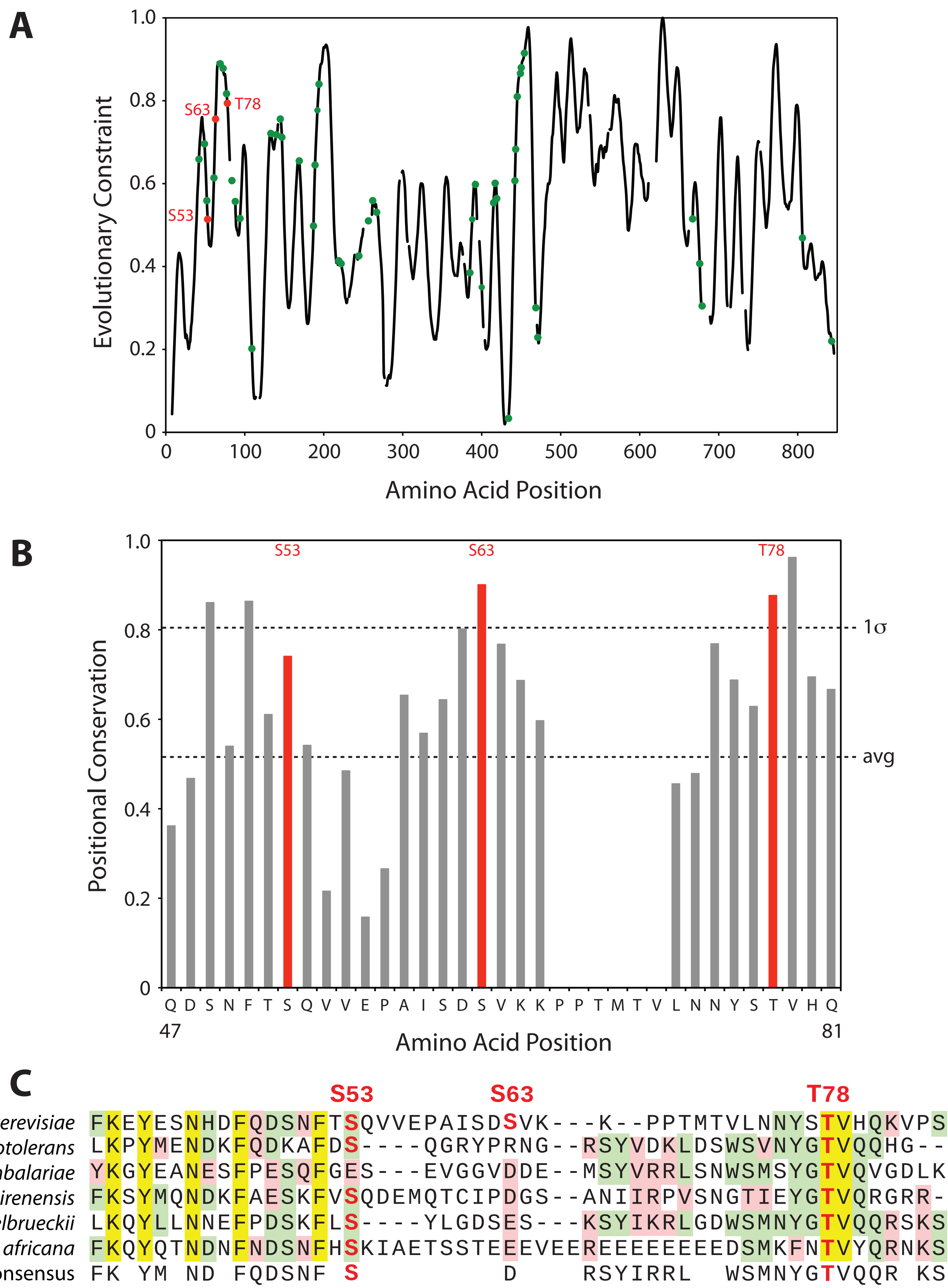
A
Evolutionary Constraint
Amino Acid Position
S63
T78
S53
1.0
0.8
0.6
0.4
0.2
0
0
100
200
300
400
500
600
700
800
B
Positional Conservation
Amino Acid Position
S53
S63
T78
1σ
avg
Q D S N F T S Q V V E P A I S D S V K K P P T M T V L N N Y S T V H Q
47
81
C
S53
S63
T78
S. cerevisiae FKEYESNHDFQDSNFTSQVVEPAISDSVK---K--PPTMTVLNNYSTVHQKVPS
L. thermotolerans LKPYMENDKFQDKAFDS----QGRYPRNG--RSYVDKLDSWSVNYGTVQQHG--
E. cymbalariae YKGYEANESFPESQFGES---EVGGVDDE--MSYVRRLSNWSMSYGTVQVGDLK
N. dairenensis FKSYMQNDKFAESKFVSQDEMQTCIPDGS--ANIIRPVSNGTIEYGTVQRGRR-
T. delbrueckii LKQYLLNNEFPDSKFLS----YLGDSES---KSYIKRLGDWSMNYGTVQQRSKS
K. africana FKQYQTNDNFNDSNFHSKIAETSSTEEEVEEREEEEEEEEDSMKFNTVYQRNKS
consensus FK YM ND FQDSNF S D RSYIRRL WSMNYGTVQQR KS

Figure S5

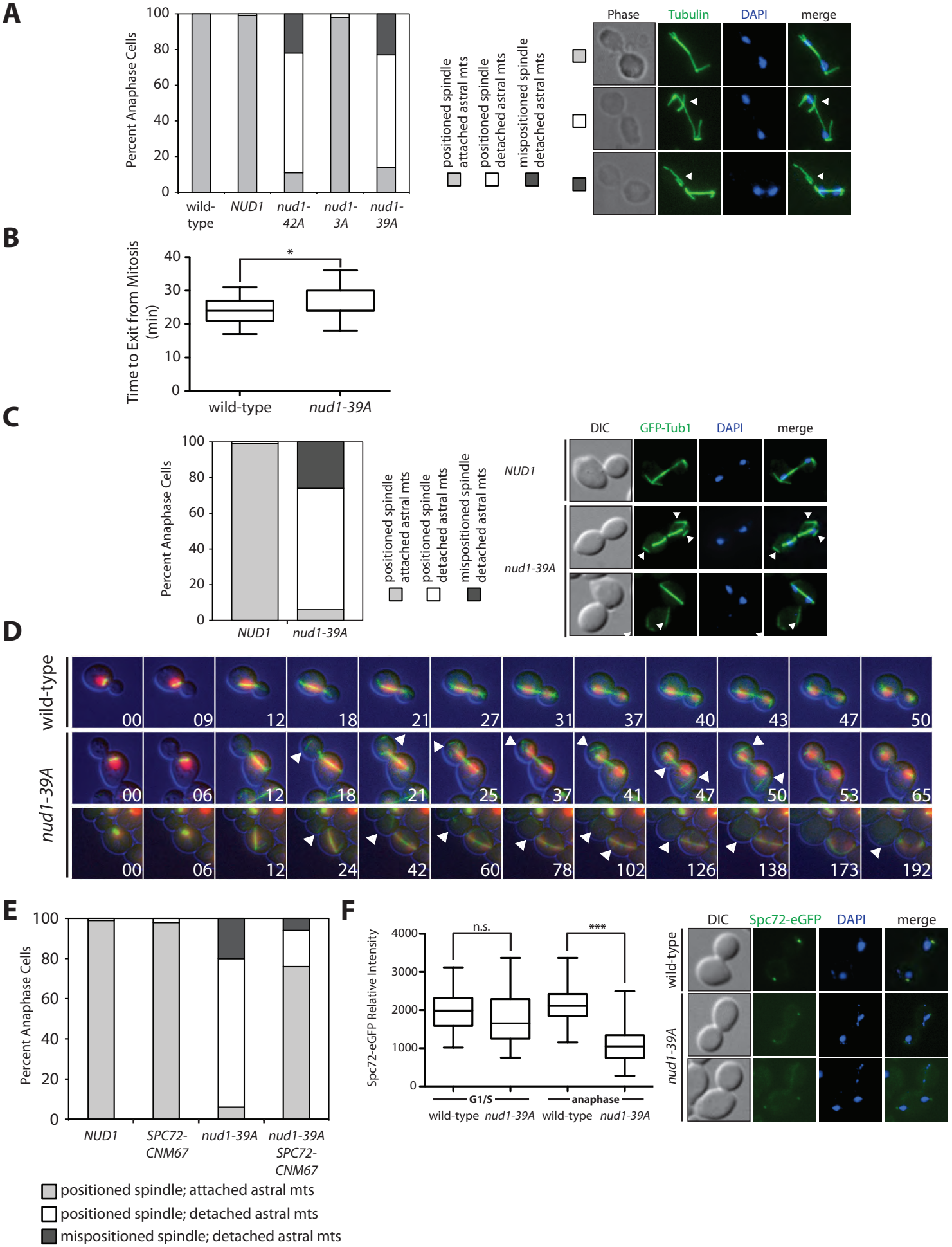
A
Percent Anaphase Cells
100
80
60
40
20
0
wild-type
NUD1
nud1-42A
nud1-3A
nud1-39A
positioned spindle attached astral mts
positioned spindle detached astral mts
mispositioned spindle detached astral mts
Phase
Tubulin
DAPI
merge
B
Time to Exit from Mitosis (min)
40
30
20
10
0
*
wild-type
nud1-39A
C
Percent Anaphase Cells
100
80
60
40
20
0
NUD1
nud1-39A
positioned spindle attached astral mts
positioned spindle detached astral mts
mispositioned spindle detached astral mts
DIC
GFP-Tub1
DAPI
merge
NUD1
nud1-39A
D
wild-type
00 09 12 18 21 27 31 37 40 43 47 50
nud1-39A
00 06 12 18 21 25 37 41 47 50 53 65
00 06 12 24 42 60 78 102 126 138 173 192
E
Percent Anaphase Cells
100
80
60
40
20
0
NUD1
SPC72-CNM67
nud1-39A
nud1-39A SPC72-CNM67
positioned spindle; attached astral mts
positioned spindle; detached astral mts
mispositioned spindle; detached astral mts
F
Spc72-eGFP Relative Intensity
4000
3000
2000
1000
0
n.s.
***
G1/S
anaphase
wild-type
nud1-39A
wild-type
nud1-39A
DIC
Spc72-eGFP
DAPI
merge
wild-type
nud1-39A

Figure S6

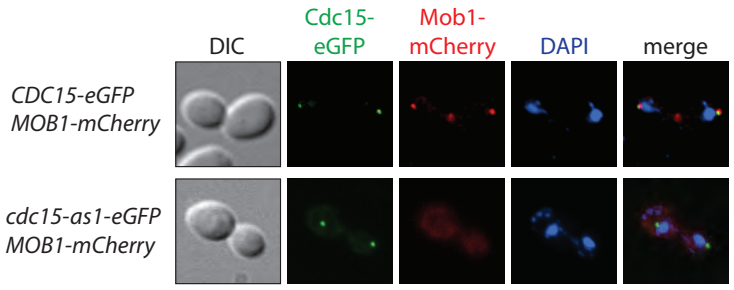
DIC
Cdc15-eGFP
Mob1-mCherry
DAPI
merge
CDC15-eGFP MOB1-mCherry
cdc15-as1-eGFP MOB1-mCherry

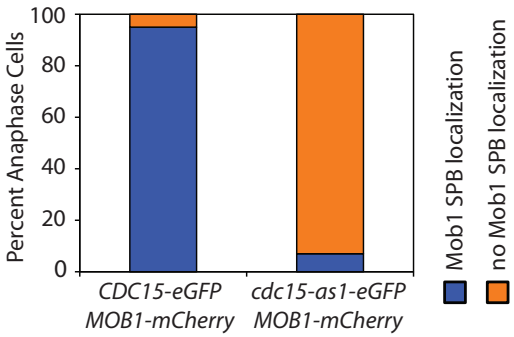
Percent Anaphase Cells
100
80
60
40
20
0
CDC15-eGFP MOB1-mCherry
cdc15-as1-eGFP MOB1-mCherry
Mob1 SPB localization
no Mob1 SPB localization

Figure S7

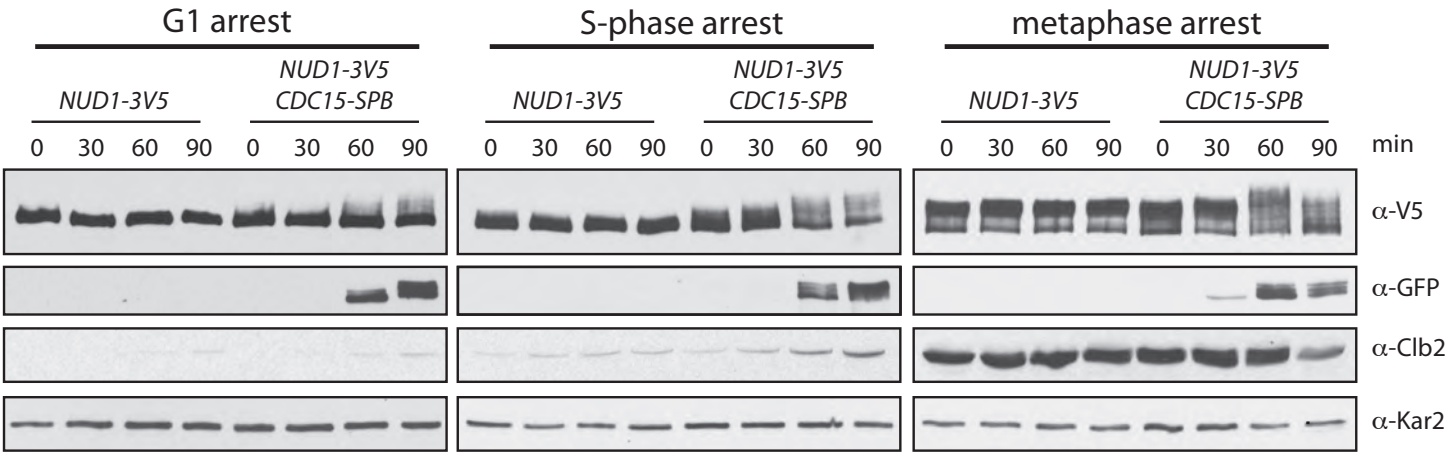
G1 arrest
S-phase arrest
metaphase arrest
NUD1-3V5
NUD1-3V5 CDC15-SPB
0 30 60 90 0 30 60 90
min
α-V5
α-GFP
α-Clb2
α-Kar2

Figure S8

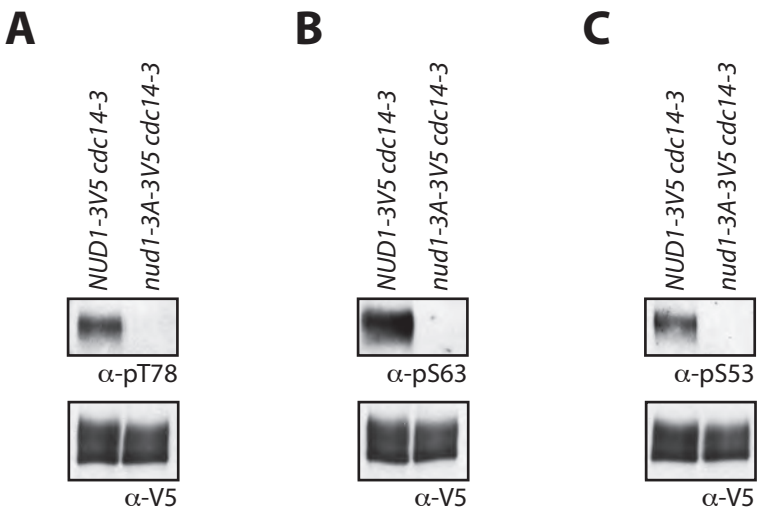
A
NUD1-3V5 cdc14-3
nud1-3A-3V5 cdc14-3
α-pT78
α-V5
B
NUD1-3V5 cdc14-3
nud1-3A-3V5 cdc14-3
α-pS63
α-V5
C
NUD1-3V5 cdc14-3
nud1-3A-3V5 cdc14-3
α-pS53
α-V5

Figure S9

A

Phospho-Threonine Peptide Motif Selection by Mob1

-4	-3	-2	-1		+1	+2	+3	+4
R (2.2)	X	Y (1.9) F (1.7)	Y (1.8) R (1.5) F (1.5) H (1.4)	pT	I (1.4) F (1.3) H (1.4)	V (2.2) I (1.7) M (1.3)	V (2.1) I (1.8)	V (2.2) I (1.7) Y (1.6) R (1.5)

B

Phospho-Serine Peptide Motif Selection by Mob1

-4	-3	-2	-1		+1	+2	+3	+4
R (1.9)	A (2.0) I (1.6) F (1.5)	F (1.4) Y (1.4)	G (1.8) Y (1.4)	pS	P (1.4)	I (1.5) F (1.4)	I (1.7) V (1.5) R (1.4) Y (1.4)	I (1.8) V (1.7) F (1.6) Y (1.5) R (1.5) L (1.5)

C

Nud1 phosphosites

	-4	-3	-2	-1		+1	+2	+3	+4
pS53	S	N	F	T	pS	Q	V	V	E
pS63	A	I	S	D	pS	V	K	K	P
pT78	N	N	Y	S	pT	V	H	Q	K

D

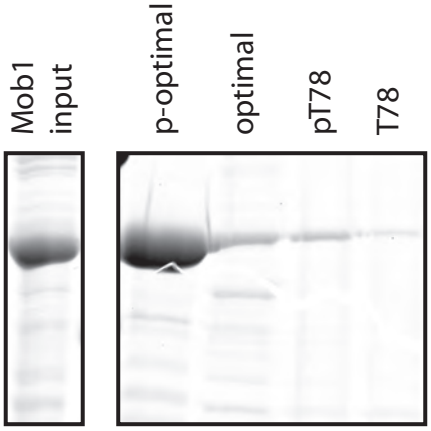

E

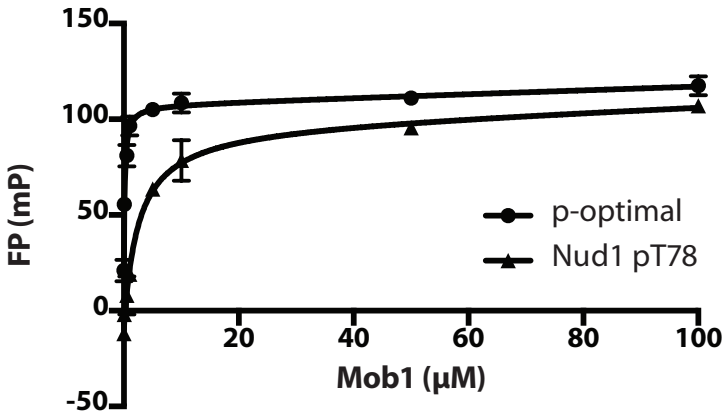

K_D p-optimal = 174 nM
K_D Nud1 pT78 = 2.4 μM

Figure S10

A

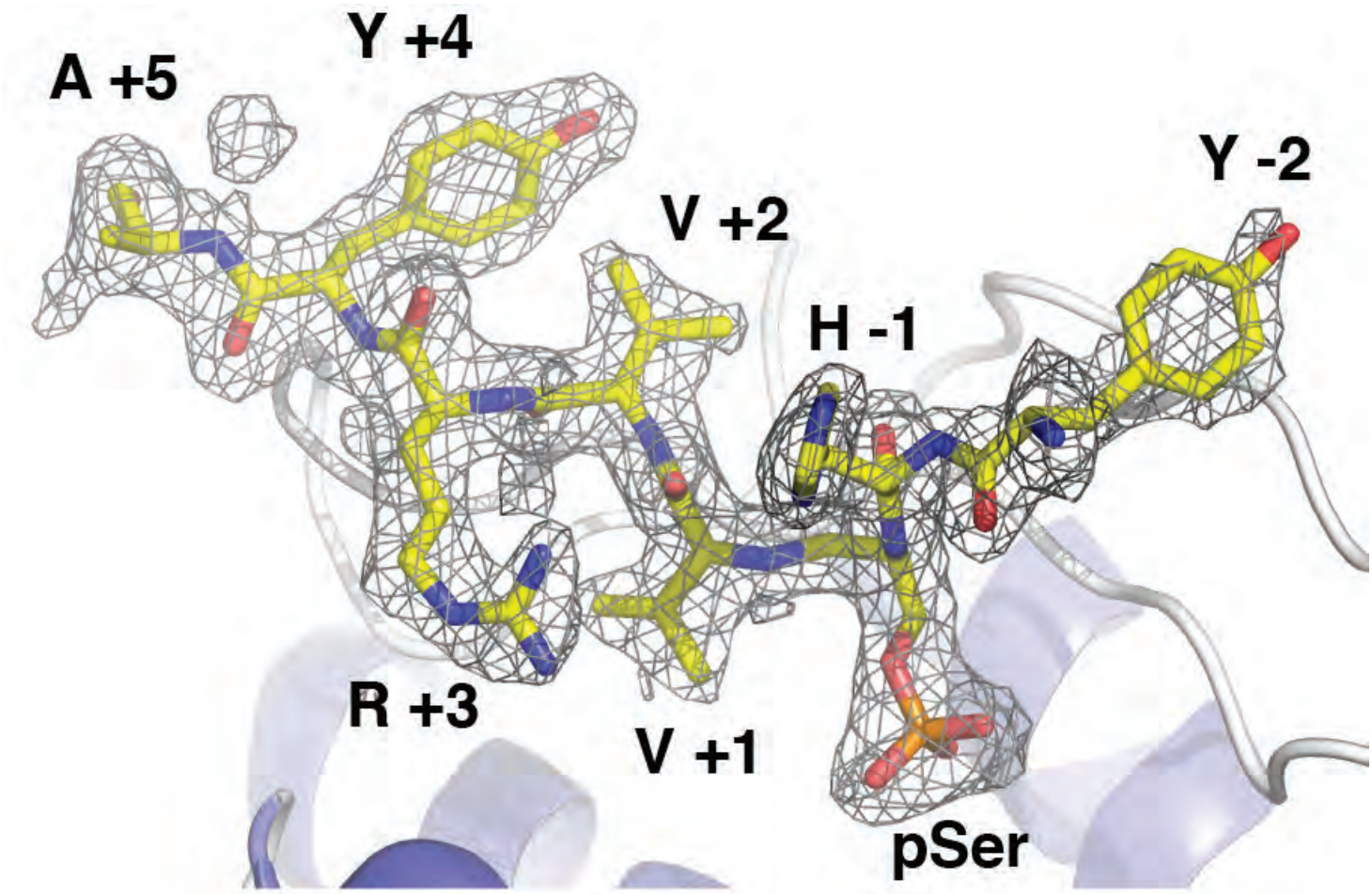

B

```
                                  * *   *
S.cerevisiae (P40484)  VIQPILRRLFRVYAHIY
S.pombe (O94360)       VIQQIFRRLFRIYAHIY
C. elegans (Q9UAX1)    ICKKILTRLFRVFVHVY
A. thaliana (Q8GYX0)   VVKTIFKRLFRVYAHIY
D. melanogaster (Q95RA8) SAKTILKRLFRVYAHIY
X. laevis (Q7T1M9)     VAKTILKRLFRVYAHIY
D. rerio (Q7ZV70)      VAKTILKRLFRVYAHIY
M. musculus (Q921Y0)   VAKTILKRLFRVYAHIY
R. norvegicus (Q3T1J9) VAKTILKRLFRVYAHIY
H. sapiens (Q9H8S9)    VAKTILKRLFRVYAHIY
Consensus              VAKTILKRLFRVYAHIY
```

Figure S11

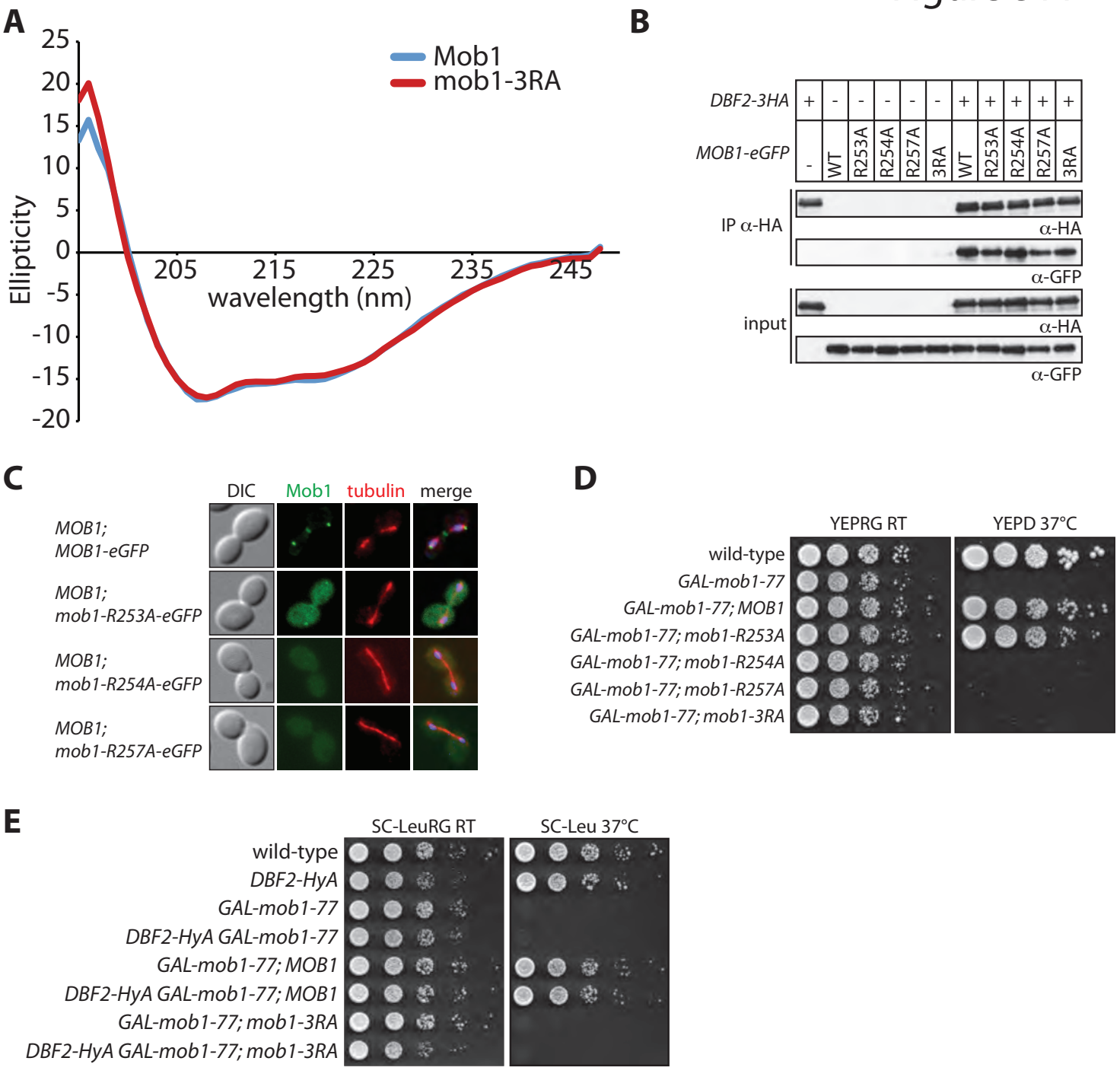
A
Mob1
mob1-3RA
Ellipticity
wavelength (nm)
25
20
15
10
5
0
-5
-10
-15
-20
205
215
225
235
245
B
DBF2-3HA
MOB1-eGFP
WT
R253A
R254A
R257A
3RA
IP α-HA
α-HA
α-GFP
input
C
DIC
Mob1
tubulin
merge
MOB1; MOB1-eGFP
MOB1; mob1-R253A-eGFP
MOB1; mob1-R254A-eGFP
MOB1; mob1-R257A-eGFP
D
YEPRG RT
YEPD 37°C
wild-type
GAL-mob1-77
GAL-mob1-77; MOB1
GAL-mob1-77; mob1-R253A
GAL-mob1-77; mob1-R254A
GAL-mob1-77; mob1-R257A
GAL-mob1-77; mob1-3RA
E
SC-LeuRG RT
SC-Leu 37°C
wild-type
DBF2-HyA
GAL-mob1-77
DBF2-HyA GAL-mob1-77
GAL-mob1-77; MOB1
DBF2-HyA GAL-mob1-77; MOB1
GAL-mob1-77; mob1-3RA
DBF2-HyA GAL-mob1-77; mob1-3RA

Figure S12

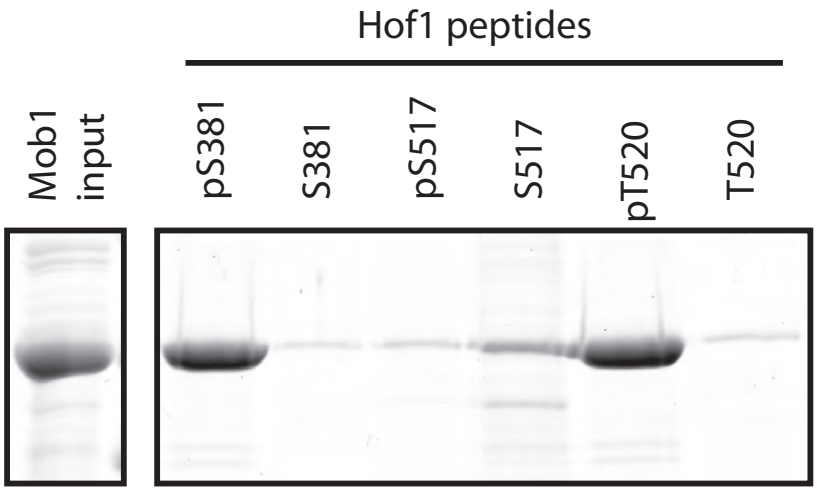

Figure S13

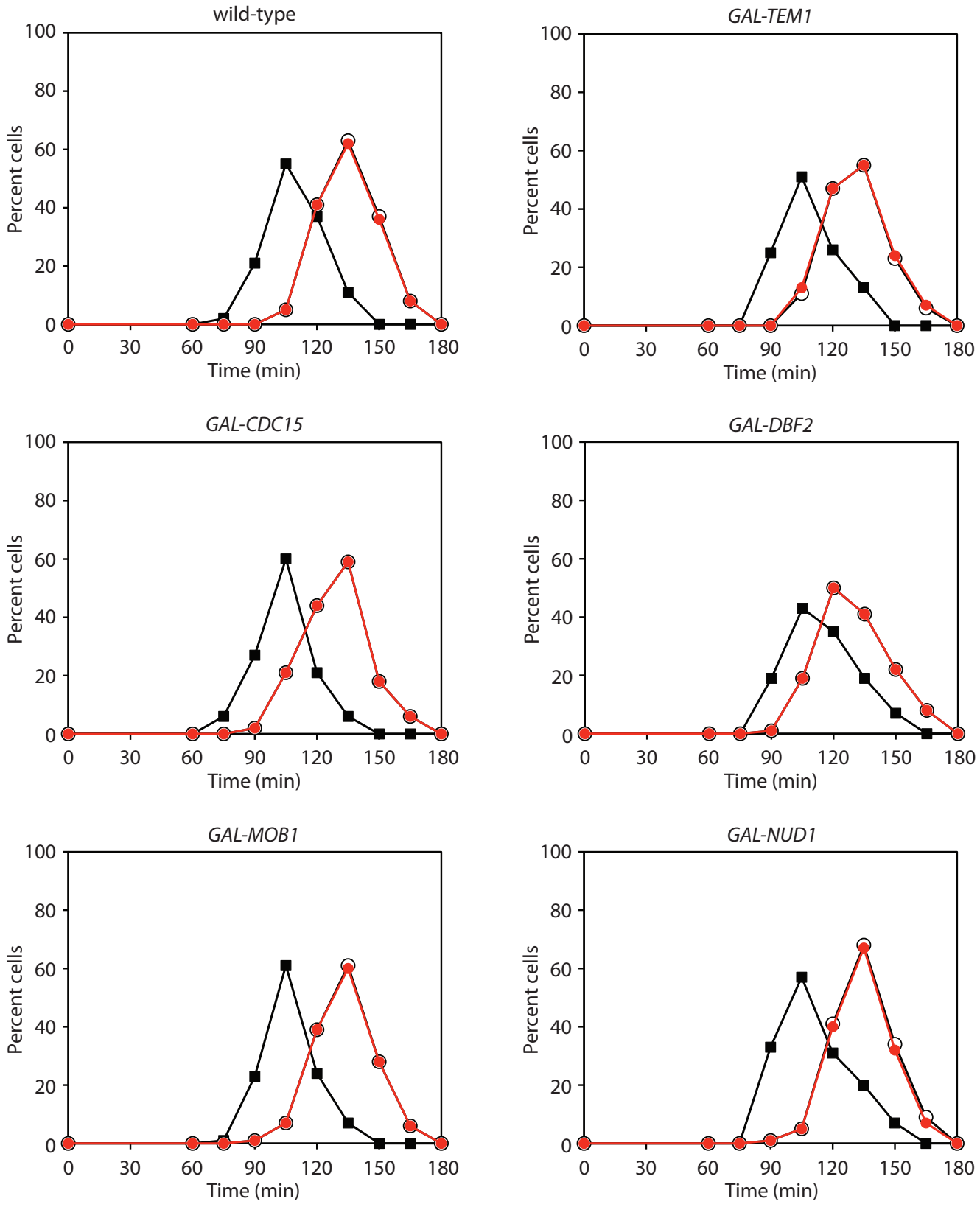
wild-type
GAL-TEM1
GAL-CDC15
GAL-DBF2
GAL-MOB1
GAL-NUD1
Percent cells
Time (min)
0
20
40
60
80
100
0
30
60
90
120
150
180
metaphase cells
anaphase cells
Cdc14 released

Figure S14

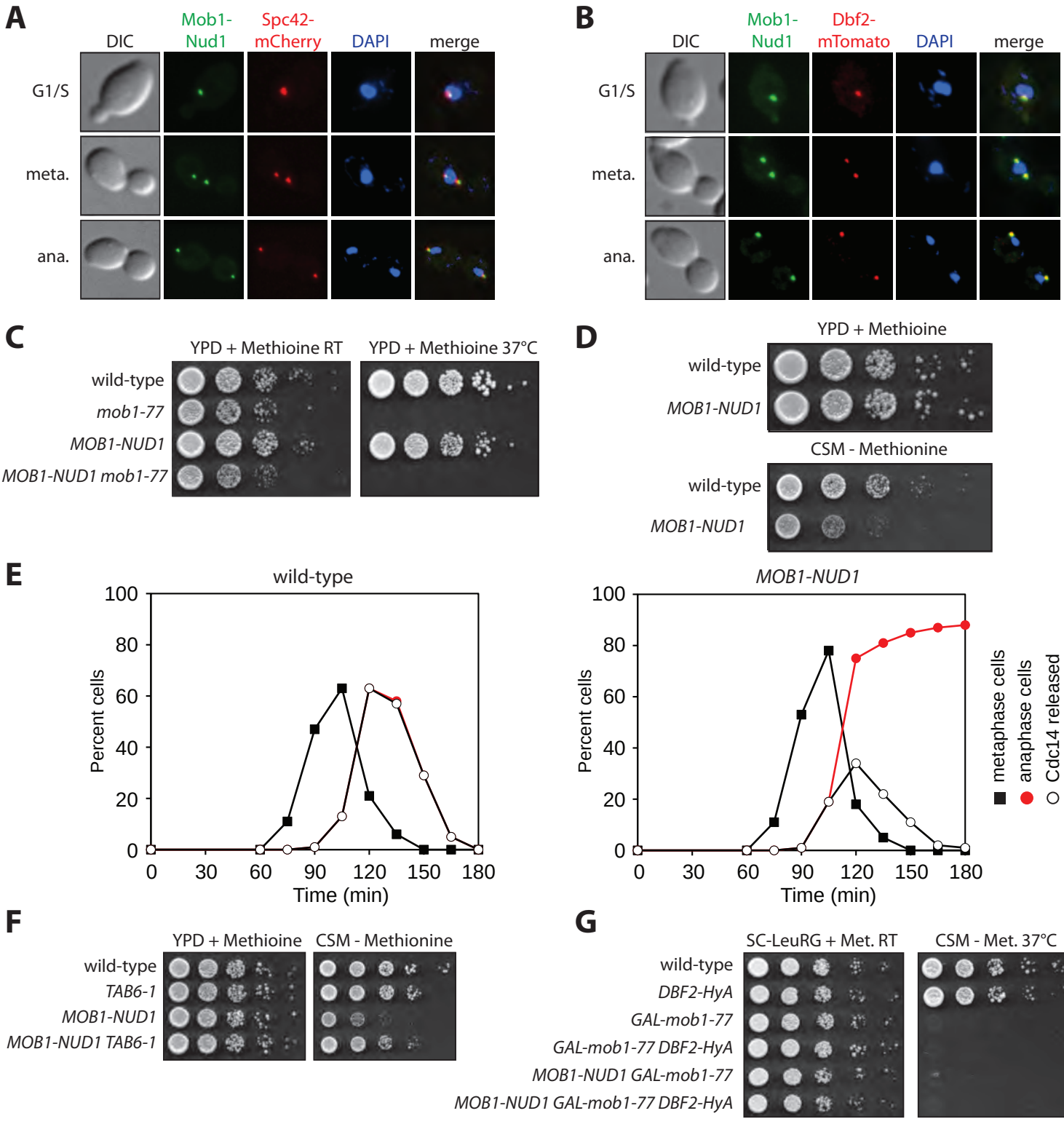
A
DIC
Mob1-Nud1
Spc42-mCherry
DAPI
merge
G1/S
meta.
ana.
B
DIC
Mob1-Nud1
Dbf2-mTomato
DAPI
merge
G1/S
meta.
ana.
C
YPD + Methioine RT
YPD + Methioine 37°C
wild-type
mob1-77
MOB1-NUD1
MOB1-NUD1 mob1-77
D
YPD + Methioine
wild-type
MOB1-NUD1
CSM - Methionine
wild-type
MOB1-NUD1
E
wild-type
MOB1-NUD1
Percent cells
Time (min)
metaphase cells
anaphase cells
Cdc14 released
F
YPD + Methioine
CSM - Methionine
wild-type
TAB6-1
MOB1-NUD1
MOB1-NUD1 TAB6-1
G
SC-LeuRG + Met. RT
CSM - Met. 37°C
wild-type
DBF2-HyA
GAL-mob1-77
GAL-mob1-77 DBF2-HyA
MOB1-NUD1 GAL-mob1-77
MOB1-NUD1 GAL-mob1-77 DBF2-HyA

Table S1. Nud1 phosphosites and *nud1* phosphomutant alleles

SPB protein	Amino Acid	Asynchronous	Mitotic	Covered	G1	Covered	*nud1-42A*	*nud1-39A*	*nud1-27A*	*nud1-3A*
Nud1	S42	S42	S42	+	S42	+	A	A	S	S
	S49		S49	+		+	A	A	A	S
	T52		T52	+	T52	+	A	A	T	T
	S53		S53	+		+	A	S	A	A
	S61		S61	+	S61	+	A	A	S	S
	S63		S63	+		+	A	S	A	A
	T71		T71	+		-	A	A	A	T
	Y76	Y76		+		-	Y	Y	Y	Y
	S77	?	S77	+		-	A	A	A	S
	T78	?	T78	+		-	A	T	A	A
	S85			+	S85	+	S	S	S	S
	S88	S88		+		+	S	S	S	S
	S94		S94	+		+	A	A	A	S
	S109	S109	S109	+		+	A	A	A	S
	S133		S133	+		+	A	A	A	S
	S140	S140	S140	+	S140	+	A	A	A	S
	T145		T145	+		+	A	A	A	T
	T147	T147		+		+	T	T	T	T
	T169		T169	+		+	A	A	A	T
	S187		S187	+		-	A	A	A	S
	S189	S189	S189	+		-	A	A	A	S
	S192	S192	S192	+		-	A	A	A	S
	S194	S194		+		-	A	A	A	S
	S219		S219	+		-	S	S	S	S
	S222	S222	S222	+		-	A	A	A	S
	S240	S240	S240	+		+	A	A	A	S
	T259		T259	+		-	A	A	A	T
	S262	S262		+		-	S	S	S	S
	S267		S267	+		-	A	A	A	S
	S385	S385	S385	+	S385	+	A	A	S	S
	T388	T388	T388	+	T388	+	A	A	T	T
	T392	T392	T392	+	T392	+	A	A	T	T
	T400		T400	+		+	A	A	A	T
	T415	T415		+		+	T	T	T	T
	S417	S417		+		+	A	A	A	S
	S419		S419	+		+	A	A	A	S
	T432	T432		+		+	T	T	T	T
	T442	T442	T442	+		+	A	A	A	T
	S443	S443	S443	+	S443	+	A	A	S	S
	S445	S445	S445	+	S445	+	A	A	S	S
	T449	T449	T449	+		+	A	A	T	T
	S450	S450	S450	+	S450	+	A	A	S	S
	T454	T454	T454	+		+	A	A	A	T
	S469	S469	S469	+	S469	+	A	A	S	S
	S471		S471	+		+	A	A	A	S
	S667			+	S667	+	S	S	S	S
	T676	T676		+		+	T	T	T	T
	S681	T681		+		+	T	T	T	T
	T806		T806	+		+	A	A	T	T
	T843		T843	+		+	A	A	T	T
							S467A	S467A	S467A	
Ambiguous Assignment	*Y359 or S363*		Y359 or S363	+		+	T805A	T805A		
Ambiguous Assignment	*S813 or S815*		S813 or S815	+		+	S815A	S815A		
Potential phosphorylation site	*S33*		S33 or T52	+		+				
Potential phosphorylation site	*Y40*		Y40 or T52	+		+				
Potential phosphorylation site	*T93*		T93 or S94	+		+				
Potential phosphorylation site	*S224*	S222 or S224		+		-				
Potential phosphorylation site	*T404*		T392 or T404	+		+				
Potential phosphorylation site	S467	S467 or S469		+		+				
Potential phosphorylation site	*T805*		T805 or T806	+		+				
Possible cell cycle observation	S77	S77 or T78								
Possible cell cycle observation	S77	S77 or T78								

Table S2. Table of Yeast Strains

A1411	*MATa, CDC14-3HA*
A2441	*MATa, GAL-TEM1::URA3*
A2546	*MATa, GAL-DBF2::TRP1*
A2587	*MATa, ade2-1, leu2-3, ura3, trp1-1, his3-11,15, can1-100, GAL, psi+*
A2747	*MATa, CDC14-3HA, DBF2-3MYC*
A3911	*MATa, DBF2-3HA::HIS3*
A4084	*MATa, GAL-CDC15::TRP1*
A5588	*MATa, GAL-NLS-9MYC-TEVProtease-NLS2::TRP1*
A18274	*MATa, kar9::HIS5*
A24513	*MATa, NUD1-3V5::KanMX6*
A24631	*MATa, MOB1-eGFP::KanMx6, ura3:pRS306-mCherry-TUB1:URA3*
A24957	*MATa, cdc14-3, GAL-CDC15-3HA::URA3*
A27353	*MATa, SPC72-eGFP::HIS3*
A27463	*MATa, NUD1-3V5::TRP1 (YIplac204)*
A27931	*MATa, HIS3Mx6::GAL-NUD1-3V5::TRP1 (YIplac204)*
A27933	*MATa, HIS3Mx6::GAL-nud1-27A-3V5::TRP1 (YIplac204)*
A28009	*MATa, HIS3Mx6::GAL-NUD1-3V5::TRP1 (YIplac204)*
A28022	*MATa, Dbf2-HyA (LEU2;pRS315)*
A28436	*MATa, TAB6-1::TRP1*
A28499	*MATa, PMET3-CDC15-eGFP-CNM67::LEU2, Mob1-mCherry::NatMX6*
A28553	*MATa, pSPC72-SPC72(1-276)-NotI-CNM67::URA3 (integrated at CNM67)*
A28650	*MATa, nud1::KanMX6, NUD1-3V5::TRP1 (YIplac204), Dbf2-HyA (LEU2;pRS315), CDC15-eGFP::KanMX6, pSPC72-SPC72(1-276)-NotI-CNM67::URA3 (integrated at CNM67), ura3::pRS306-mCherry-TUB1::URA3*
A29128	*MATa, nud1-42A-3V5::TRP1 (YIplac204)*
A29239	*MATa, His3MX6::GAL-nud1-42A-3V5::TRP1 (YIplac204)*
A29248	*MATa, KanMX6::GAL-3HA-nud1-44::TRP1, nud1::HIS5*
A29412	*MATa, nud1::KanMX6, NUD1-3V5::TRP1 (YIplac204), Dbf2-HyA (LEU2;pRS315), pSPC72-SPC72(1-276)-NotI-CNM67::URA3 (integrated at CNM67)*
A29450	*MATa, nud1::KanMX6, NUD1-3V5::TRP1 (YIplac204), Dbf2-HyA (LEU2;pRS315), pSPC72-SPC72(1-276)-NotI-CNM67::URA3 (integrated at CNM67), ura3::pRS306-mCherry-TUB1::URA3, MOB1-eGFP::KanMx6*
A29453	*MATa, nud1::KanMX6, NUD1-3V5::TRP1 (YIplac204), ura3::pRS306-mCherry-TUB1::URA3, MOB1-eGFP::KanMx6*
A29500	*MATa, KanMX6::GAL-3HA-nud1-44::TRP1, nud1::HIS5, nud1-42A-3V5::LEU2 (YIplac128)*
A29506	*MATa, nud1::KanMX6, nud1-42A-3V5::TRP1 (YIplac204), Dbf2-HyA (LEU2;pRS315), CDC15-eGFP::KanMX6, pSPC72-SPC72(1-276)-NotI-CNM67::URA3 (integrated at CNM67), ura3::pRS306-mCherry-TUB1::URA3*
A29508	*MATa, nud1::KanMX6, nud1-42A-3V5::TRP1 (YIplac204), Dbf2-HyA (LEU2;pRS315), pSPC72-SPC72(1-276)-NotI-CNM67::URA3 (integrated at CNM67), ura3::pRS306-mCherry-TUB1::URA3*
A29679	*MATa, nud1::KanMX6, nud1-42A-3V5::TRP1 (YIplac204), Dbf2-HyA (LEU2;pRS315), pSPC72-SPC72(1-276)-NotI-CNM67::URA3 (integrated at CNM67), ura3::pRS306-mCherry-TUB1::URA3, Tem1-GFP:HisMx6*

A29682	*MATa, nud1::KanMX6, nud1-42A-3V5::TRP1 (YIplac204), Dbf2-HyA (LEU2;pRS315), pSPC72-SPC72(1-276)-NotI-CNM67::URA3 (integrated at CNM67), ura3::pRS306-mCherry-TUB1::URA3, DBF2-eGFP::His3MX6*
A29685	*MATa, KanMX6::GAL-3HA-nud1-44::TRP1, nud1::HIS5, NUD1-3V5::LEU2 (YIplac128)*
A29711	*MATa, nud1::KanMX6, NUD1-3V5::TRP1 (YIplac204), Dbf2-HyA (LEU2;pRS315), pSPC72-SPC72(1-276)-NotI-CNM67::URA3 (integrated at CNM67), ura3::pRS306-mCherry-TUB1::URA3, DBF2-eGFP::His3MX6*
A29722	*MATa, nud1::KanMX6, nud1-42A-3V5::TRP1 (YIplac204), Dbf2-HyA (LEU2;pRS315), pSPC72-SPC72(1-276)-NotI-CNM67::URA3 (integrated at CNM67), ura3::pRS306-mCherry-TUB1::URA3, MOB1-eGFP::KanMx6*
A29730	*MATa, nud1::KanMX6, nud1-42A-3V5::TRP1 (YIplac204), Dbf2-HyA (LEU2;pRS315), pSPC72-SPC72(1-276)-NotI-CNM67::URA3 (integrated at CNM67), ura3::pRS306-mCherry-TUB1::URA3, BFA1-yEGFP::KanMX*
A29733	*MATa, nud1::KanMX6, NUD1-3V5::TRP1 (YIplac204), Dbf2-HyA (LEU2;pRS315), pSPC72-SPC72(1-276)-NotI-CNM67::URA3 (integrated at CNM67), ura3::pRS306-mCherry-TUB1::URA3, BFA1-yEGFP::KanMX*
A29851	*MATa, MOB1-3HA::His3MX6, NUD1-3V5::KanMX6, cdc14-3*
A29878	*MATa, NUD1-3V5::LEU2 (YIplac128), nud1::HIS5, KanMX6::GAL-3HA-nud1-44::TRP1, CDC14-3HA, DBF2-3MYC*
A29881	*MATa, nud1-42A-3V5::LEU2 (YIplac128), nud1::HIS5, KanMX6::GAL-3HA-nud1-44::TRP1, CDC14-3HA, DBF2-3MYC*
A29899	*MATa, nud1::KanMX6, NUD1-3V5::TRP1 (YIplac204), Dbf2-HyA (LEU2;pRS315), pSPC72-SPC72(1-276)-NotI-CNM67::URA3 (integrated at CNM67), ura3::pRS306-mCherry-TUB1::URA3, Tem1-GFP:HisMx6*
A29921	*MATa, DBF2-eGFP::His3MX6, ura3::pRS306-mCherry-TUB1::URA3*
A30371	*MATa, GAL-cdc15-K54L::URA3, cdc14-3*
A30611	*MATa, HIS3MX6::GAL-nud1-20A-3V5::TRP1 (YIplac204)*
A30614	*MATa, HIS3MX6::GAL-nud1-16A; NUD1-3V5::TRP1 (YIplac204)*
A30617	*MATa, HIS3MX6::GAL-nud1-12A-3V5::TRP1 (YIplac204)*
A30620	*MATa, HIS3MX6::GAL-nud1-8A; NUD1-3V5::TRP1 (YIplac204)*
A30623	*MATa, HIS3MX6::GAL-nud1-7A-3V5::TRP1 (YIplac204)*
A30649	*MATa, HIS3MX6::GAL-nud1-6A-3V5::TRP1 (YIplac204)*
A30652	*MATa, HIS3MX6::GAL-nud1-4A-3V5::TRP1 (YIplac204)*
A30655	*MATa, HIS3MX6::GAL-nud1-S49A,S53A,S63A-3V5::TRP1 (YIplac204)*
A30913	*MATa, HIS3MX6::GAL-nud1-21A-3V5::TRP1 (YIplac204)*
A30915	*MATa, HIS3MX6::GAL-nud1-24A-3V5::TRP1 (YIplac204)*
A30917	*MATa, HIS3MX6::GAL-nud1-25A-3V5::TRP1 (YIplac204)*
A30925	*MATa, HIS3Mx6::GAL-nud1-T78A-3V5::TRP1 (YIplac204)*
A31089	*MATa, Mob1-mCherry::NatMX6, CDC15-eGFP::KanMX6*
A31169	*MATa, nud1::KanMX6, nud1-S53A,S63A,T78A-3V5::TRP1 (YIplac204), Dbf2-HyA (LEU2;pRS315), ura3::pRS306-mCherry-TUB1::URA3, MOB1-eGFP::KanMx6*
A31176	*MATa, HIS3MX6::GAL-nud1-23A-3V5::TRP1 (YIplac204)*
A31209	*MATa, HIS3Mx6::GAL-nud1-S53A,T78A-3V5::TRP1 (YIplac204)*
A31211	*MATa, HIS3Mx6::GAL-nud1-S63A,T78A-3V5::TRP1 (YIplac204)*
A31215	*MATa, HIS3Mx6::GAL-nud1-S53A,S63A,T78A-3V5::TRP1 (YIplac204)*
A31355	*MATa, cdc15::CDC15-as1 (L99G)-eGFP::KANMX6, Mob1-mCherry::NatMX6*
A31388	*MATa, nud1::KanMX6, nud1-39A-3V5::TRP1 (YIplac204)*
A31422	*MATa, NUD1-3V5::KanMX6, PMET3-CDC15-eGFP-CNM67::LEU2*

A31466	*MATa, SPC72-eGFP::HIS3, nud1::KanMX6, nud1(39A)-3V5::TRP1 (YIplac204)*
A31472	*MATa, ura3::pAFS125-TUB1p-GFPTUB1::URA3, nud1::KanMX6, nud1-39A-3V5::TRP1 (YIplac204)*
A31477	*MATa, MOB1-eGFP::KanMx6, ura3:pRS306-mCherry-TUB1:URA3, nud1::KanMX6, nud1-39A-3V5::TRP1 (YIplac204)*
A31479	*MATa, mob1-77*
A31500	*MATa, MOB1-eGFP (YIplac204), ura3::pRS306-mCherry-TUB1::URA3*
A31502	*MATa, MOB1-eGFP (YIplac204), DBF2-3HA::HIS3*
A31504	*MATa, mob1-R253A,R254A,R257A-eGFP (YIplac204), ura3::pRS306-mCherry-TUB1::URA3*
A31506	*MATa, mob1-R253A,R254A,R257A-eGFP (YIplac204), DBF2-3HA::HIS3*
A31548	*MATa, MOB1-eGFP (YIplac204)*
A31550	*MATa, mob1-R253A,R254A,R257A-eGFP (YIplac204)*
A31602	*MATalpha, MOB1-6HA::His3MX6, NUD1-3V5::KanMX6, cdc14-3*
A31661	*MATa, NUD1-3V5::KanMX6, MOB1-6HA::His3MX6, cdc14-3, cdc15-2*
A31728	*MATa, mob1-R253A-eGFP (YIplac204)*
A31730	*MATa, mob1-R254A-eGFP (YIplac204)*
A31732	*MATa, mob1-R257A-eGFP (YIplac204)*
A31893	*MATa, mob1-R253A-eGFP (YIplac204), ura3::pRS306-mCherry-TUB1::URA3*
A31895	*MATa, mob1-R254A-eGFP (YIplac204), ura3::pRS306-mCherry-TUB1::URA3*
A31897	*MATa, mob1-R257A-eGFP (YIplac204), ura3::pRS306-mCherry-TUB1::URA3*
A31901	*MATa, mob1-R253A-eGFP (YIplac204), DBF2-3HA::HIS3*
A31905	*MATa, mob1-R254A-eGFP (YIplac204), DBF2-3HA::HIS3*
A31909	*MATa, mob1-R257A-eGFP (YIplac204), DBF2-3HA::HIS3*
A31966	*MATa, nud1::KanMX6, nud1-39A-3V5::TRP1 (YIplac204), kar9::HIS5*
A32241	*MATa, nud1::KanMX6, NUD1-3V5::TRP1 (YIplac204), ura3::pAFS125-TUB1p-GFPTUB1::URA3*
A32289	*MATa, PMET3-MOB1-TEV-eGFP-NUD1::URA3*
A32292	*MATa, nud1-S53A,S63A,T78A-3V5::LEU2 (YIplac128), KanMX6::GAL-3HA-nud1-44::TRP1, nud1::HIS5*
A32295	*MATa, nud1-39A-3V5::LEU2 (YIplac128), KanMX6::GAL-3HA-nud1-44::TRP1, nud1::HIS5*
A32336	*MATa, PMET3-MOB1-eGFP-NUD1::URA3*
A32452	*MATa, KANMX6::GAL-mob1-77*
A32483	*MATa, nud1::KanMX6, NUD1-3V5::TRP1 (YIplac204), Dbf2-HyA (LEU2;pRS315), cdc14-3*
A32507	*MATa, nud1::KanMX6, nud1-S53A,S63A,T78A-3V5::TRP1 (YIplac204), Dbf2-HyA (LEU2;pRS315), cdc14-3*
A32551	*MATa, KANMX6::GAL-mob1-77, Dbf2-HyA (LEU2;pRS315)*
A32586	*MATa, KANMX6::GAL-mob1-77, MOB1-eGFP (YIplac204)*
A32589	*MATa, KANMX6::GAL-mob1-77, mob1-R253A,R254A,R257A-eGFP (YIplac204)*
A32592	*MATa, KANMX6::GAL-mob1-77, mob1-R253A-eGFP (YIplac204)*
A32595	*MATa, KANMX6::GAL-mob1-77, mob1-R254A-eGFP (YIplac204)*
A32598	*MATa, KANMX6::GAL-mob1-77, mob1-R257A-eGFP (YIplac204)*
A32612	*MATa, GAL-MOB1::LEU2*
A32624	*MATa, PMET3-MOB1-eGFP-NUD1::URA3, SPC42-mCherry:KanMx6*

A32635	*MATa, PMET3-MOB1-eGFP-NUD1::URA3, mob1-77*
A32654	*MATa, DBF2-eGFP::His3MX6, ura3::pRS306-mCherry-TUB1::URA3, KANMX6::GAL-mob1-77*
A32661	*MATa, PMET3-MOB1-eGFP-CNM67::URA3, TAB6-1::TRP1*
A32667	*MATa, PMET3-MOB1-eGFP-NUD1::URA3, CDC14-3HA, DBF2-3MYC*
A32668	*MATa, PMET3-MOB1-eGFP-NUD1::URA3, CDC14-3HA*
A32674	*MATa, KANMX6::GAL-mob1-77, MOB1-eGFP (YIplac204), Dbf2-HyA (pRS315)*
A32676	*MATa, KANMX6::GAL-mob1-77, mob1-R253A,R254A,R257A-eGFP (YIplac204), Dbf2-HyA (pRS315)*
A32715	*MATa, PMET3-MOB1-eGFP-NUD1::URA3, Dbf2-HyA (LEU2;pRS315)*
A32730	*MATa, pRS306-pCTS1-2xmCherry-SV40NLS::URA3 (integrated at CTS1), ura3::pAFS125-TUB1p-GFPTUB1::URA3 (integrated at URA3), nud1::KanMX6, nud1-39A-3V5::TRP1 (YIplac204)*
A32731	*MATa, pRS306-pCTS1-2xmCherry-SV40NLS::URA3 (integrated at CTS1), ura3::pAFS125-TUB1p-GFPTUB1::URA3 (integrated at URA3)*
A32793	*MATa, pSPC72-SPC72(1-276)-NotI-CNM67::URA3 (integrated at CNM67), ura3::pAFS125-TUB1p-GFPTUB1::URA3, nud1::KanMX6, nud1-39A-3V5::TRP1 (YIplac204)*
A32796	*MATa, pSPC72-SPC72(1-276)-NotI-CNM67::URA3 (integrated at CNM67), ura3::pAFS125-TUB1p-GFPTUB1::URA3*
A32797	*MATa, Dbf2-tdTomato::KanMX6, PMET3-MOB1-eGFP-NUD1::URA3*
A32818	*MATa, KANMX6::GAL-mob1-77, MOB1-eGFP (YIplac204), DBF2-3MYC*
A32823	*MATa, KANMX6::GAL-mob1-77, mob1-R253A,R254A,R257A-eGFP (YIplac204), DBF2-3MYC*
A32881	*MATa, KANMX6::GAL-mob1-77, Dbf2-HyA (LEU2;pRS315), PMET3-MOB1-eGFP-NUD1::URA3*
A32888	*MATalpha, pSPC72-SPC72(1-276)-NotI-CNM67::URA3 (integrated at CNM67), nud1::KanMX6, nud1-39A-3V5::TRP1 (YIplac204), kar9::HIS5*
A32979	*MATa, pRS315 (CEN, LEU2)*
A32986	*MATa, KANMX6::GAL-mob1-77, pRS315 (CEN, LEU2)*
A32988	*MATa, KANMX6::GAL-mob1-77, MOB1-eGFP (YIplac204), pRS315 (CEN, LEU2)*
A32990	*MATa, KANMX6::GAL-mob1-77, mob1-R253A,R254A,R257A-eGFP (YIplac204), pRS315 (CEN, LEU2)*
A32992	*MATa, PMET3-MOB1-eGFP-NUD1::URA3, KANMX6::GAL-mob1-77, pRS315 (CEN, LEU2)*
A33283	*MATa, GAL-NLS-9MYC-TEVProtease-NLS2::TRP1, PMET3-MOB1-TEV-eGFP-NUD1::URA3, CDC14-3HA*
A33285	*MATa, GAL-NLS-9MYC-TEVProtease-NLS2::TRP1, PMET3-MOB1-TEV-eGFP-NUD1::URA3*
A33287	*MATa, PMET3-MOB1-TEV-eGFP-NUD1::URA3, CDC14-3HA*
A33291	*MATa, GAL-NLS-9MYC-TEVProtease-NLS2::TRP1, CDC14-3HA*
A33549	*MATa, GAL-NLS-9MYC-TEVProtease-NLS2::TRP1, PMET3-MOB1-eGFP-NUD1::URA3, CDC14-3HA*
A33551	*MATa, GAL-NLS-9MYC-TEVProtease-NLS2::TRP1, PMET3-MOB1-eGFP-NUD1::URA3*

Table S3. Table of Plasmids

pA1358	pRS306-*GFP-TUB1*
pA1420	pRS306-*CTS1-2xmCherry-SV40NLS*
pA1469	pRS306-*mCherry-TUB1*
pA1842	pRS315-*Dbf2-HyA*
pA1880	YIplac204-*PMET3-CDC15-eGFP-CNM67*
pA1921	YIplac204-*NUD1-3V5*
pA1931	YIplac204-*nud1-27A-3V5*
pA1998	YIplac204-*nud1-42A-3V5*
pA2056	YIplac204-*nud1-T78A-3V5*
pA2086	YIplac204-*nud1-S53A,T78A-3V5*
pA2088	YIplac204-*nud1-S63A,T78A-3V5*
pA2096	YIplac204-*nud1-S53A,S63A,T78A-3V5*
pA2111	pGEX6p1-*GST-NUD1(aa1-150)*
pA2117	YIplac204-*nud1-39A-3V5*
pA2122	pGEX6p1-*GST-nud1-S53A,S63A,T78A (aa1-150)*
pA2124	YIplac204-*MOB1-eGFP*
pA2126	YIplac204-*mob1-R253A,R254A,R257A-eGFP*
pA2165	YIplac204-*mob1-R253A-eGFP*
pA2167	YIplac204-*mob1-R254A-eGFP*
pA2169	YIplac204-*mob1-R257A-eGFP*
pA2186	YIplac128-*nud1-S53A,S63A,T78A-3V5*
pA2192	YIplac211-*MET3-MOB1-eGFP-NUD1*
pA2248	pET28a-*His6-GST-mob1-R253A,R254A,R257A (aa79-314)*

Table S4 - Crystallographic Statistics

Data collection	$P2_1$
Space group	
Unit cell (Å)	a = 34.5, b = 59.6, c = 53.4
	β=104.7°
Number of molecules/au	1
Wavelength (Å)	0.9795
Resolution (Å)	60 – 2.1 (2.2 – 2.1)
Completeness (%)	88.0 (52.8)
Total observations	35662
Unique observations	10903
Redundancy	3.1 (2.1)
R_{merge}[a] (%)	5.7 (28.0)
< I/σ (I) >	11.7 (2.8)
Structure Solution	
Phasing method	Molecular replacement
Search model	1PI1
Refinement	
Resolution (Å)	40 – 2.1
N_{ref}[b]	10057
R_{work} (%)[c]	17.8
R_{free} (%)	22.6
r.m.s.d. bond lengths ($Å^2$)	0.003
r.m.s.d. bond angles (°)	0.74
Ramachandran plot	
Preferred regions (%)	98.0
Allowed regions (%)	2.0
Outliers (%)	0.0
<B> protein ($Å^2$)	48.9
<B> peptide ($Å^2$)	39.7

[a] $R_{merge} = \Sigma_h\Sigma_i|I_{h,i} - \langle I_h\rangle| / \Sigma_h\Sigma_i I_{h,i}$, where $I_{h,i}$ is the intensity of the individual reflections and $\langle I_h\rangle$ is the mean intensity over symmetrically equivalent reflections.

[b] N_{ref} is the number of reflections used in refinement.

[c] $R_{work} = \Sigma_h||F_{o,h}| - |F_{c,h}||/\Sigma_h|F_{o,h}|$, where $|F_{o,h}|$ and $|F_{c,h}|$ are observed and calculated structure factor amplitudes, respectively; R_{free} was calculated with 5% of the data.